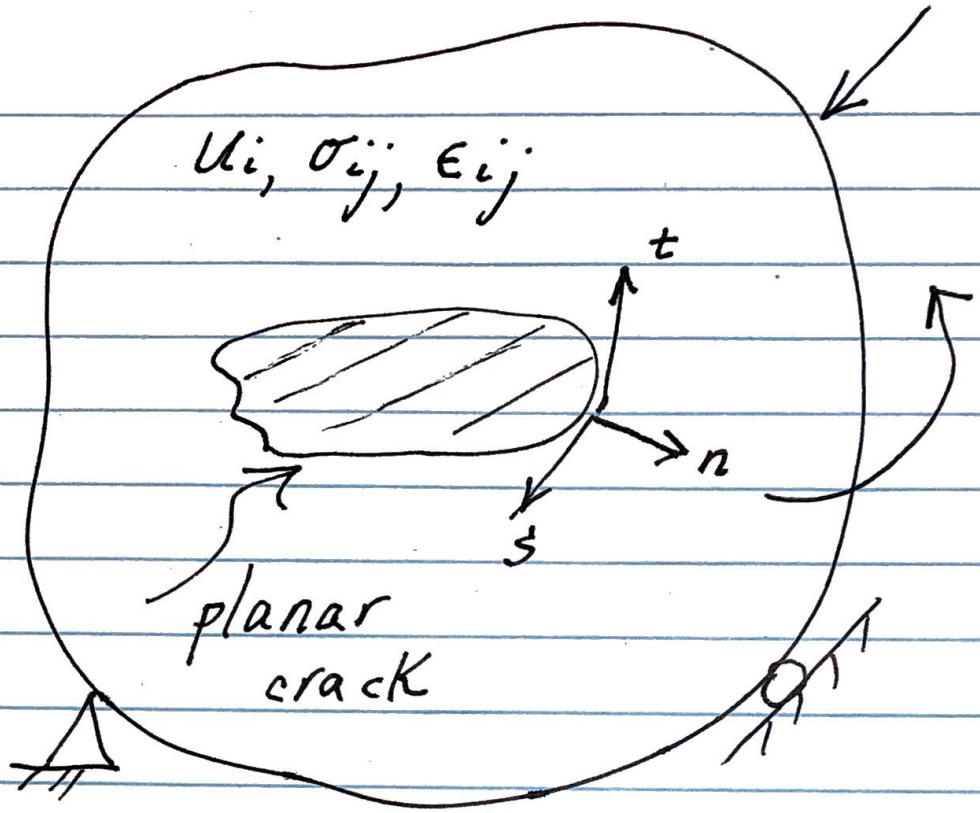

$$\frac{\partial \sigma_{ji}}{\partial x_j} + f_i = 0, \quad \sigma_{ij} = \sigma_{ji} \quad \text{(Equilibrium)}$$

$$\epsilon_{ij} = \frac{1}{2}\left(\frac{\partial u_i}{\partial x_j} + \frac{\partial u_j}{\partial x_i}\right) \quad \text{(strain-displacement)}$$

$$\sigma_{ij} = 2\mu\left(\epsilon_{ij} + \frac{\nu}{1-2\nu}\epsilon_{kk}\delta_{ij}\right) \quad \text{(Hookes law)}$$

$$R_{ij} = \epsilon_{ipq}\epsilon_{jrs}\epsilon_{qs,pr} = 0 \quad \text{(local compatibility)}$$

+ Boundary conditions

It can be shown that at distance "r" which is much smaller than other characteristic lengths, such as the crack length:

1) the stress, strain and displacement fields have a "universal" form and are combinations of plane and anti-plane forms in terms of the associated stress intensity factors, K_I, K_{II}, K_{III}

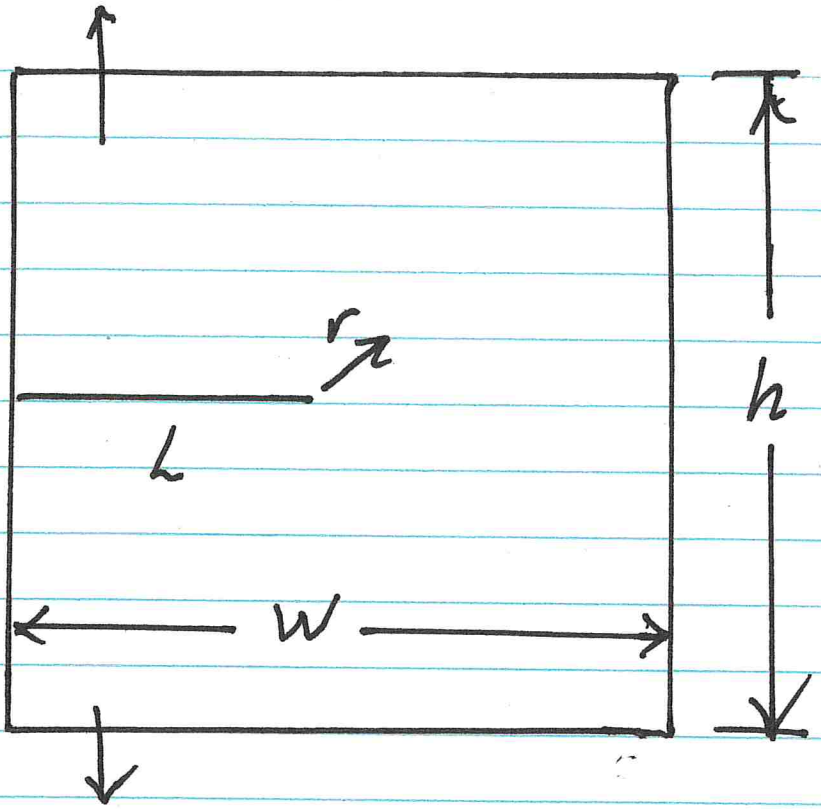

Zoom in at a point very close to crack tip, $\frac{r}{L}, \frac{r}{(W-L)}, \frac{r}{h} \ll 1$

The crack looks infinite in length!

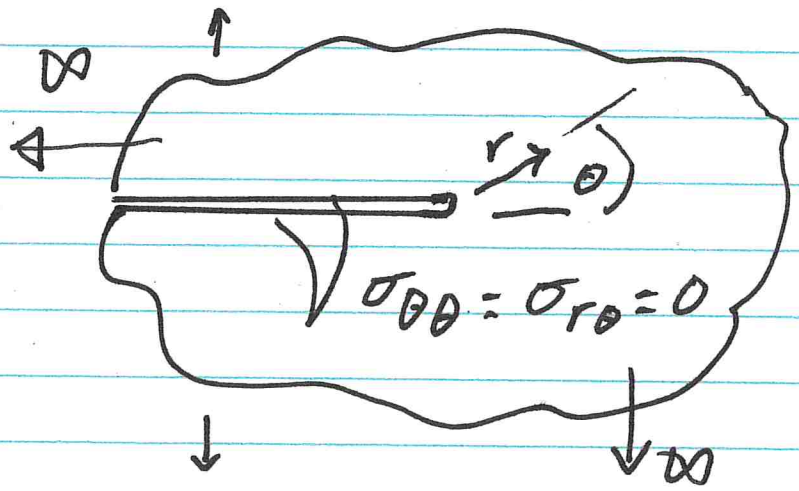

We do not consider the details in the far-field

We will learn that for each mode of loading, near the tip the form of σ_{ij}, ε_{ij}, u_i does not depend on configuration and loading type:

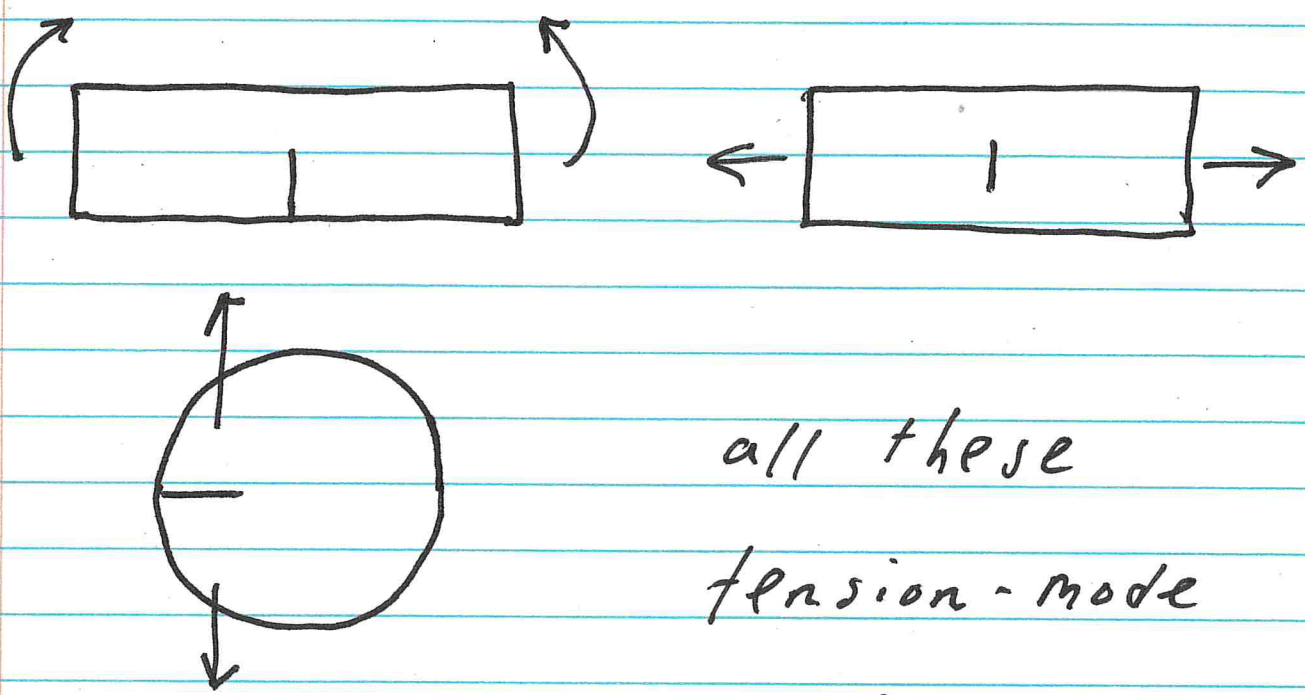

all these tension-mode specimens have the same forms of σ_{ij} at small r!!

$$\sigma_{ij} = \frac{K_I}{\sqrt{2\pi r}} f_{ij}^{I}(\theta) + \frac{K_{II}}{\sqrt{2\pi r}} f_{ij}^{II}(\theta) + \frac{K_{III}}{\sqrt{2\pi r}} f_{ij}^{III}(\theta) + \text{H.O.T.}$$

$\int_{\text{bounded}}$

Mode I:

$$\begin{Bmatrix} \sigma_{xx} \\ \sigma_{xy} \\ \sigma_{yy} \end{Bmatrix} = \frac{K_I}{\sqrt{2\pi r}} \cos\frac{\theta}{2} \begin{Bmatrix} 1 - \sin\theta/2 \sin 3\theta/2 \\ \sin\theta/2 \cos 3\theta/2 \\ 1 + \sin\theta/2 \sin 3\theta/2 \end{Bmatrix}$$

$$\begin{Bmatrix} u_x \\ u_y \end{Bmatrix} = \frac{K_I}{2\mu} \sqrt{\frac{r}{2\pi}} \begin{Bmatrix} \cos\theta/2 \left[\kappa - 1 + 2\sin^2\theta/2\right] \\ \sin\theta/2 \left[\kappa + 1 - 2\cos^2\theta/2\right] \end{Bmatrix}$$

$$\kappa = \begin{cases} 3 - 4\nu, & \text{plane strain} \\ \frac{3-\nu}{1+\nu}, & \text{plane stress} \end{cases}$$

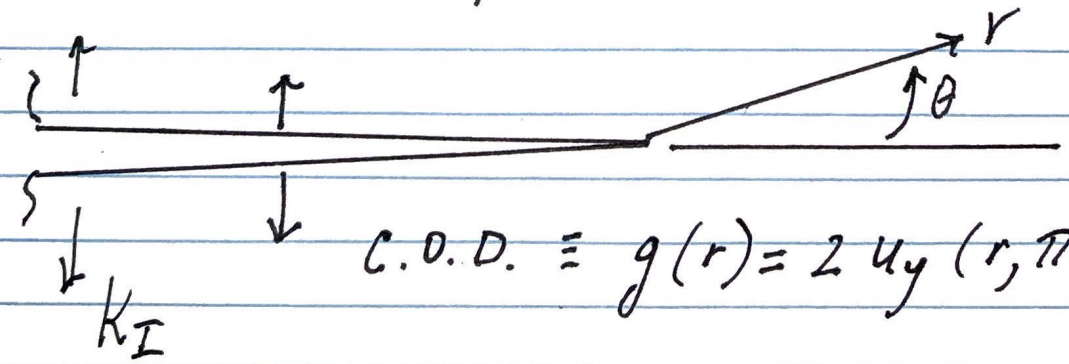

C.O.D. $\equiv g(r) = 2u_y(r, \pi)$

For convenience employ a polar coordinate system

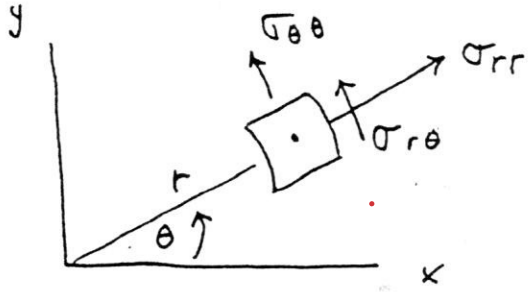

$x = r\cos\theta$
$y = r\sin\theta$
$x^2 + y^2 = r^2$
$\tan\theta = y/x$

Stresses are $\sigma_{rr}, \sigma_{r\theta}, \sigma_{\theta\theta}$
Displ. are u_r, u_θ

Equilibrium:

$$\frac{\partial \sigma_{rr}}{\partial r} + \frac{1}{r}\frac{\partial \sigma_{r\theta}}{\partial \theta} + \frac{\sigma_{rr} - \sigma_{\theta\theta}}{r} = 0 \qquad (r)$$

$$\frac{\partial \sigma_{r\theta}}{\partial r} + \frac{1}{r}\frac{\partial \sigma_{\theta\theta}}{\partial \theta} + 2\frac{\sigma_{r\theta}}{r} = 0 \qquad (\theta)$$

Strain-displacement:

$$\epsilon_{rr} = \frac{\partial u_r}{\partial r}$$

$$\epsilon_{\theta\theta} = \frac{u_r}{r} + \frac{1}{r}\frac{\partial u_\theta}{\partial \theta}$$

$$\epsilon_{r\theta} = \frac{1}{2}\left\{ \frac{1}{r}\frac{\partial u_r}{\partial \theta} + \frac{\partial u_\theta}{\partial r} - \frac{u_\theta}{r} \right\}$$

Compatibility:

$$\nabla^2(\sigma_{rr} + \sigma_{\theta\theta}) = \left(\frac{\partial^2}{\partial r^2} + \frac{1}{r}\frac{\partial}{\partial r} + \frac{1}{r^2}\frac{\partial^2}{\partial \theta^2}\right)(\sigma_{rr} + \sigma_{\theta\theta}) = 0$$

Hooke's Law: G E, ν

$$\sigma_{r\theta} = 2\mu \epsilon_{r\theta}$$

$$\sigma_{rr} = \mu \left\{ \frac{3-\chi}{\chi-1} \epsilon_{\theta\theta} + \frac{\chi+1}{\chi-1} \epsilon_r \right\} \qquad (1)$$

$$\sigma_{\theta\theta} = \mu \left\{ \frac{3-\chi}{\chi-1} \epsilon_{rr} + \frac{\chi+1}{\chi-1} \epsilon_\theta \right\}$$

$$\chi = \begin{cases} 3 - 4\nu & \text{plane strain} \\ \frac{3-\nu}{1+\nu} & \text{plane stress} \end{cases}$$

Airy Stress Function:

$$\sigma_{\theta\theta} = \frac{\partial^2 U}{\partial r^2} \qquad \sigma_{rr} = \frac{1}{r}\frac{\partial U}{\partial r} + \frac{1}{r^2}\frac{\partial^2 U}{\partial \theta^2} \qquad (2)$$

$$\sigma_{r\theta} = \frac{-\partial}{\partial r}\left(\frac{1}{r}\frac{\partial U}{\partial \theta}\right)$$

again BIHARMONIC

$$\nabla^4 U = 0 \qquad (3)$$

A general solution to the biharmonic equation can be written the form

Atronomer Royal George Biddell Airy (1801-1892)

Lucasian Professor at Cambridge
President of the Royal Society of London

Scientific contributions include:

•Improved orbital theory of Venus and the Moon.
•Computation of the density of the earth by swinging a pendulum at the top and the bottom of a deep mine.
•Fluid dynamics: theories of waves and tides.
•A mathematical study of the rainbow.

SIR GEORGE BIDDELL AIRY.

George Biddell Airy (1801-1892)
presented his paper
to the Royal Society in 1862

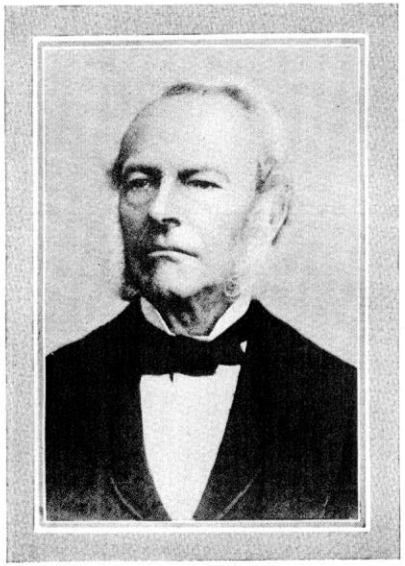

Sir George Gabriel Stokes

George Gabriel Stokes
Subsequently sent
the paper to James Clerk Maxwell
and someone else for review.

James Clerk Maxwell.

Maxwell recommended publication
And also named the stress function
After Airy. But he also
raised some issues with
Airy's solutions and suggested
improvements that were discussed
in a series of letters between himself,
Stokes and Airy.

$$\Delta\Delta\phi = 0$$

Airy's original paper presented solutions for the stresses in a finite rectangular beam treated as a two-dimensional problem of elasticity.

Why would an astronomer be concerned with the elasticity of plates and beams?

Note that the deflection, w, of a plate is governed by

$$\Delta\Delta w = q/D$$

where q is the transverse loading distribution and D is the flexural rigidity.

At the beginning of the 1860's Airy built for the Observatory a new large meridian line with a telescope having an 8-inch object lens. The weight of the lens, if not accounted for, can cause inadmissible errors in observations, such as the 2 arc seconds associated with the Paris Observatory.

$U \equiv \phi$

Williams Solution:

$$\Delta\Delta\phi(r,\theta) = 0$$

try $\quad \phi = r^{\lambda+1} f(\theta)$

$$\Delta\phi = \frac{\partial^2\phi}{\partial r^2} + \frac{1}{r}\frac{\partial\phi}{\partial r} + \frac{1}{r^2}\frac{\partial^2\phi}{\partial r^2}$$

$$= r^{\lambda-1}\underbrace{\left[f'' + (\lambda+1)^2 f \right]}_{\equiv g}$$

$$\Delta\Delta\phi = \Delta\left[r^{\lambda-1} g\right] = r^{\square}\left[\frac{d^2}{d\theta^2} + (\lambda-1)^2\right]\left[\frac{d^2}{d\theta^2} + (\lambda+1)^2\right] f = 0$$

$\vdots$ steps

$$f(\theta) = e^{b\theta}$$

$$\left\{ b^2 + (\lambda-1)^2 \right\}\left\{ b^2 + (\lambda+1)^2 \right\} = 0$$

$$b = \pm (\lambda-1)i, \ \pm (\lambda+1)i$$

$$f(\theta) = A\cos(\lambda+1)\theta + B\cos(\lambda-1)\theta + C\sin(\lambda+1)\theta + D\sin(\lambda-1)\theta$$

Consider Mode-I

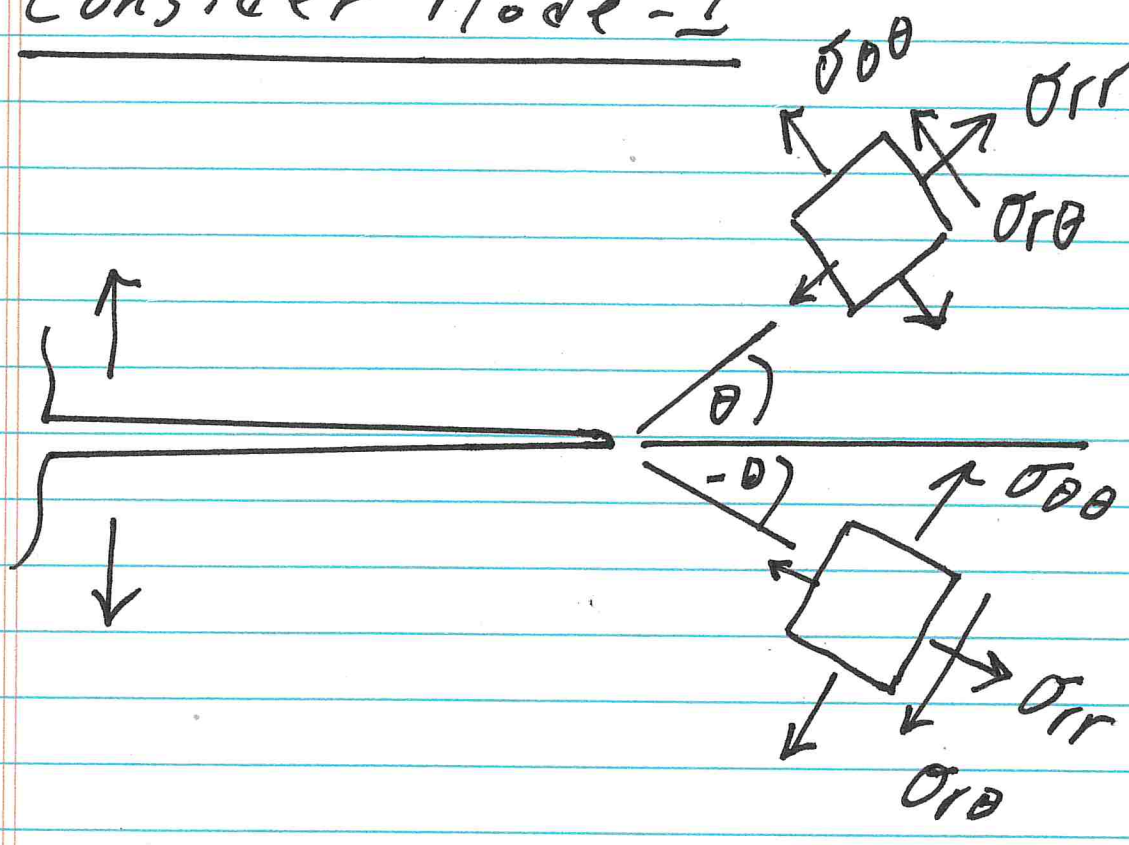

$$\sigma_{rr}(+\theta) = \sigma_{rr}(-\theta)$$

$$\sigma_{\theta\theta}(+\theta) = \sigma_{\theta\theta}(-\theta)$$

$$\sigma_{r\theta}(+\theta) = -\sigma_{r\theta}(-\theta)$$

$$u_r(+\theta) = u_r(-\theta)$$

$$u_r(+\theta) = -u_r(-\theta)$$

$\therefore C = D = 0$

$$\phi = r^{\lambda+1}\left\{A\cos(\lambda+1)\theta + B\cos(\lambda-1)\theta\right\}$$

$$\sigma_{\theta\theta} = \frac{\partial^2\phi}{\partial r^2} = \lambda(\lambda+1)r^{\lambda-1}\left[A\cos(\lambda+1)\theta + B\cos(\lambda-1)\theta\right]$$

$$\sigma_{r\theta} = \frac{-\partial}{\partial r}\left(\frac{1}{r}\frac{\partial\phi}{\partial r}\right) = \lambda r^{\lambda-1}\left[(\lambda+1)A\sin(\lambda+1)\theta + (\lambda-1)B\sin(\lambda-1)\theta\right]$$

Traction is zero along crack surfaces: $\sigma_{\theta\theta} = \sigma_{r\theta} = 0$ along $\theta = \pi$

$$\begin{bmatrix} \lambda(\lambda+1)\cos\lambda\pi & \lambda(\lambda+1)\cos\lambda\pi \\ \lambda(\lambda+1)\sin\lambda\pi & \lambda(\lambda-1)\sin\lambda\pi \end{bmatrix} \begin{Bmatrix} A \\ B \end{Bmatrix} = \begin{Bmatrix} 0 \\ 0 \end{Bmatrix}$$

$$\lambda^2 (1+\lambda) \sin(2\lambda\pi) = 0$$

$$\lambda = \ldots, -1, -1/2, 0, 1/2, 1, 3/2, \ldots$$

Interested in possible singular stresses:

$$(\sigma_{ij} \sim r^{\lambda-1})$$

look for $\lambda - 1 < 0$!!

$$\lambda < 1$$

But cannot accept infinite strain energy!!

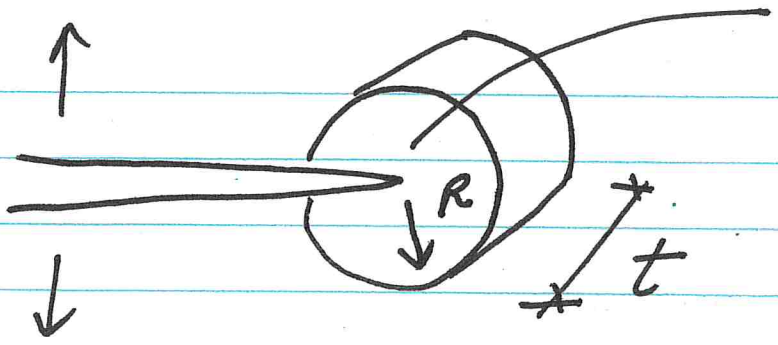

u = strain energy density

$\sim \frac{1}{2}\sigma_{ij}\varepsilon_{ij}$

Strain energy

$$\int_V u\,dV = 2\int_0^{\pi}\int_0^{R} \underbrace{r^{(2\lambda-2)}}_{r^{2\lambda-1}}\, r\,dr\,d\theta$$

$< \infty$!!

$2\lambda - 1 > -1$

$$\boxed{\lambda > 0}$$

only allowable is $\lambda = 1/2$

$\sigma \sim r^{-1/2}$!!

For $\lambda = 1/2$

$$\frac{1}{2}\left(\frac{1}{2}+1\right)\sin\frac{\pi}{2}A + \frac{1}{2}\left(\frac{1}{2}-1\right)\sin\frac{\pi}{2}B = 0$$

$$\boxed{B = 3A}$$

Substituting:

$$\sigma_{\theta\theta} = \frac{B}{\sqrt{r}}\,\frac{1}{4}\left[\cos\frac{3\theta}{2} + 3\cos\frac{\theta}{2}\right]$$

Irwin defined $K_I \equiv \sqrt{2\pi}\,B$

$$\begin{Bmatrix}\sigma_{\theta\theta}\\ \sigma_{r\theta}\\ \sigma_{rr}\end{Bmatrix} = \frac{K_I}{4\sqrt{2\pi r}}\begin{Bmatrix}\cos\frac{3\theta}{2} + 3\cos\frac{\theta}{2}\\ \sin\frac{3\theta}{2} + \sin\frac{\theta}{2}\\ -\cos\frac{3\theta}{2} + 5\cos\frac{\theta}{2}\end{Bmatrix} + H.O.T.$$

$$\sigma_{ij} = \frac{K_I}{\sqrt{2\pi r}} f_{ij}^{I}(\theta) + \frac{K_{II}}{\sqrt{2\pi r}} f_{ij}^{II}(\theta) + \frac{K_{III}}{\sqrt{2\pi r}} f_{ij}^{III}(\theta) + \text{H.O.T.}$$

$\int_{\text{bounded}}$

Mode I:

$$\begin{Bmatrix} \sigma_{xx} \\ \sigma_{xy} \\ \sigma_{yy} \end{Bmatrix} = \frac{K_I}{\sqrt{2\pi r}} \cos\frac{\theta}{2} \begin{Bmatrix} 1 - \sin\theta/2 \sin 3\theta/2 \\ \sin\theta/2 \cos 3\theta/2 \\ 1 + \sin\theta/2 \sin 3\theta/2 \end{Bmatrix}$$

$$\begin{Bmatrix} u_x \\ u_y \end{Bmatrix} = \frac{K_I}{2\mu} \sqrt{\frac{r}{2\pi}} \begin{Bmatrix} \cos\theta/2 \left[\kappa - 1 + 2\sin^2\theta/2\right] \\ \sin\theta/2 \left[\kappa + 1 - 2\cos^2\theta/2\right] \end{Bmatrix}$$

$$\kappa = \begin{cases} 3 - 4\nu, & \text{plane strain} \\ \frac{3-\nu}{1+\nu}, & \text{plane stress} \end{cases}$$

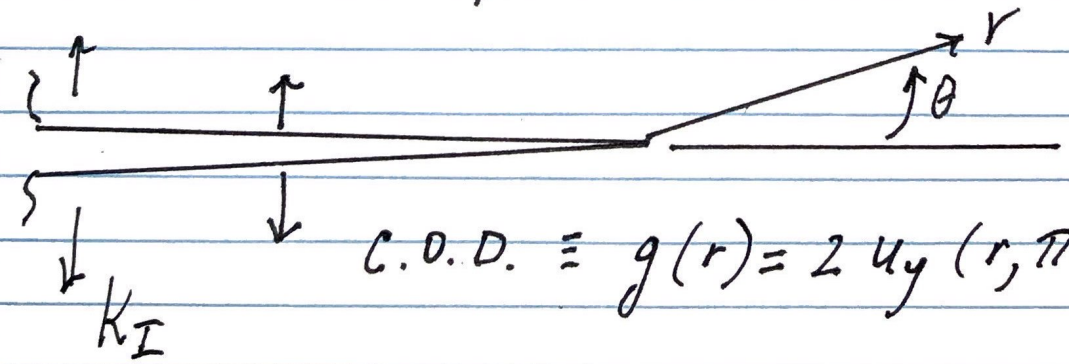

C.O.D. $\equiv g(r) = 2u_y(r, \pi)$

K_I depends on details of loading & geometry!

ex.

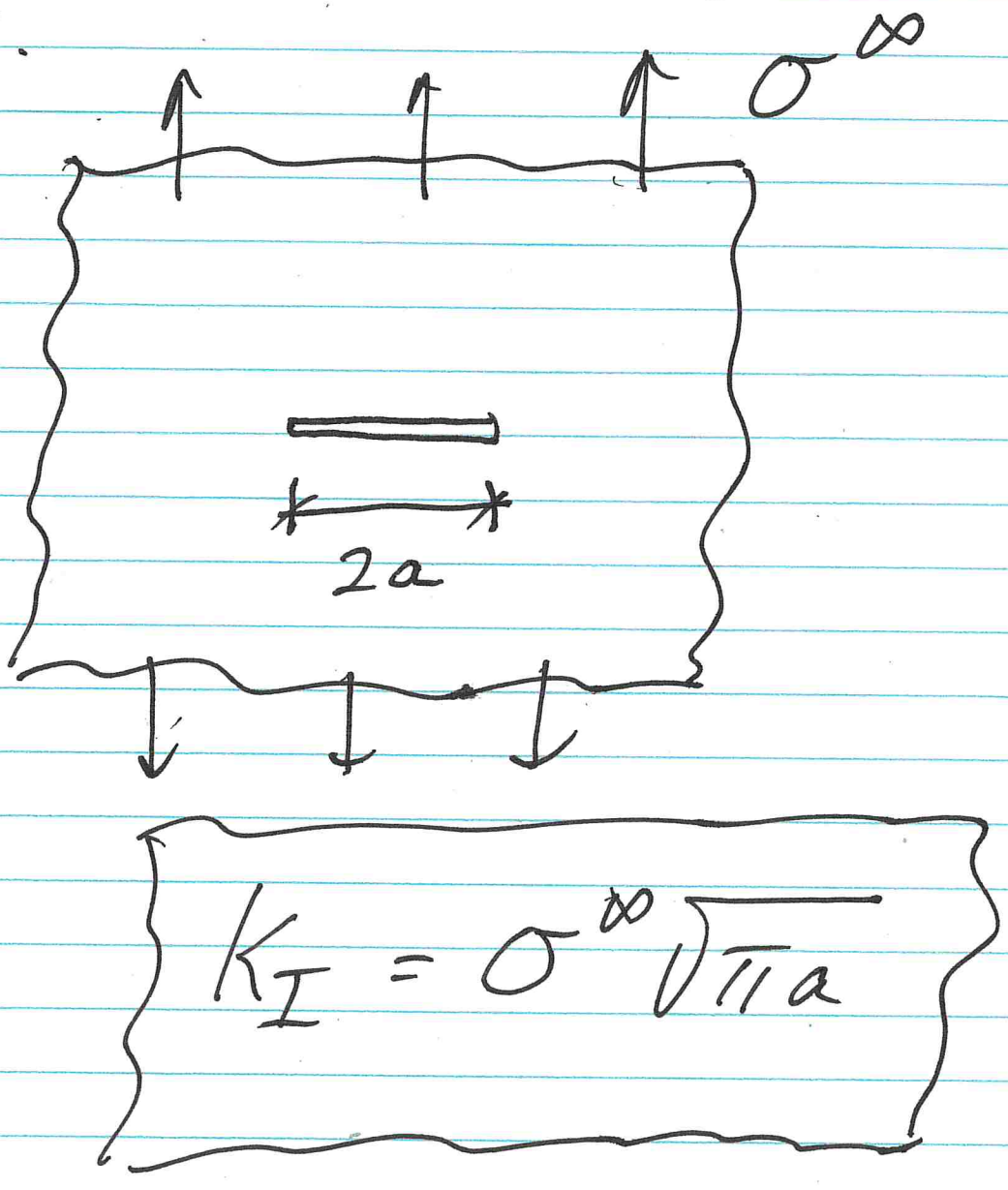

Vito Volterra

Vito Volterra

Born	3 May 1860 Ancona, Papal States
Died	11 October 1940 (aged 80) Rome, Kingdom of Italy
Nationality	Italian
Alma mater	University of Pisa
Known for	Theory of integral equations The Lotka–Volterra equations
Awards	ForMemRS[1]
Scientific career	
Fields	Mathematics
Institutions	University of Turin
Doctoral advisor	Enrico Betti
Doctoral students	Paul Lévy Joseph Pérès

Carlo Somigliana

Born	20 September 1860 Como, Italy
Died	20 June 1955 (aged 94) Casanova Lanza, Italy
Nationality	Italian
Alma mater	Scuola Normale Superiore di Pisa
Known for	Somigliana identity
Scientific career	
Fields	Mathematical physics Theory of elasticity Glaciology
Doctoral advisor	Eugenio Beltrami

John D. Eshelby

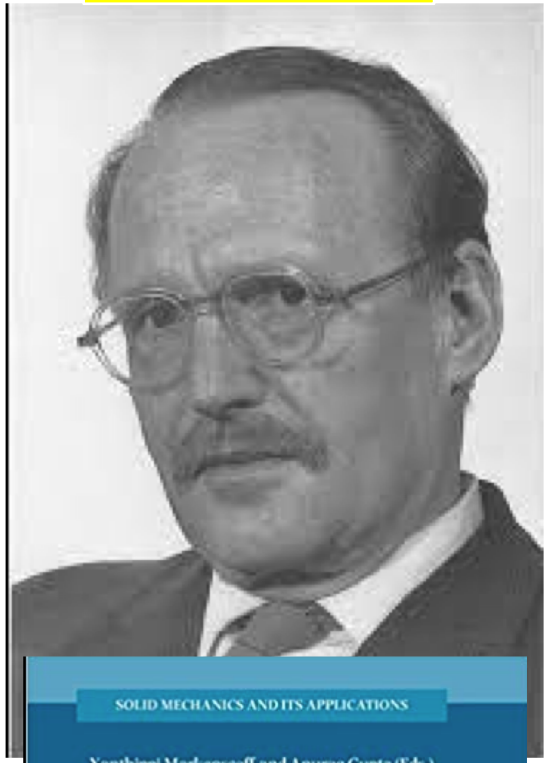

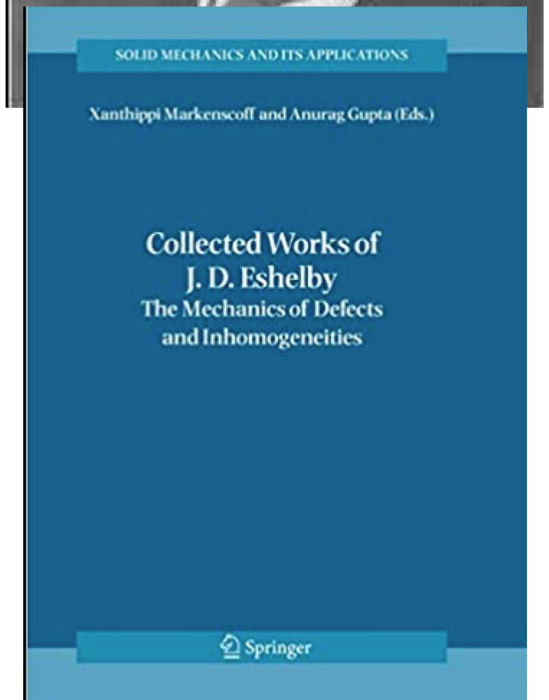

John Dundurs (Northwestern Univ.)

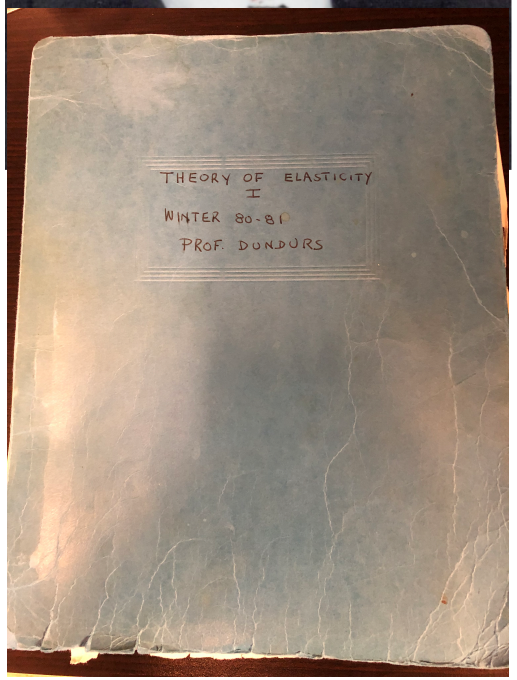

Vito Volterra

From Wikipedia, the free encyclopedia

Professor **Vito Volterra** KBE FRS(For) HFRSE (/vɒlˈtɛrə/, Italian: [ˈviːto volˈtɛrra]; 3 May 1860 – 11 October 1940) was an Italian mathematician and physicist, known for his contributions to mathematical biology and integral equations,[2][3] being one of the founders of functional analysis.[4]

Carlo Somigliana

From Wikipedia, the free encyclopedia

Carlo Somigliana (20 September 1860 – 20 June 1955) was an Italian mathematician and a classical mathematical physicist, faithful member of the school of Enrico Betti and Eugenio Beltrami.[1][2] He made important contributions to linear elasticity: the Somigliana integral equation, analogous to Green's formula in potential theory, and the Somigliana dislocations are named after him. Other fields he contribute to include seismic wave propagation, gravimetry and glaciology.[3] One of his ancestors was Alessandro Volta:[4] precisely, the great Como physicist was an ancestor of Carlo's mother, Teresa Volta.[5]

John D. Eshelby

From Wikipedia, the free encyclopedia

John Douglas Eshelby FRS (21 December 1916 – 10 December 1981) was a scientist in micromechanics. His work has shaped the fields of defect mechanics and micromechanics of inhomogeneous solids for fifty years and provided the basis for the quantitative analysis of the controlling mechanisms of plastic deformation and fracture.

Fundamental Solutions of the Plane Problem

Introduction to the Concept of Dislocation

Two analytical solutions that are useful in formulating boundary value problems involving cracks are the point force and edge dislocation in an infinitely extended medium. For simplicity the discussion is restricted to the ***plane*** problems shown in Figure 3: the concentrated force per unit thickness F (Figure 3a) and the discrete edge dislocation b (Figure 3b), which is represented by the symbol $\perp$. The extension to three dimensional problems is described briefly in Chapter 3. Because they are associated with a concentrated ***action*** at a point, the force and dislocation solutions are the Green's functions for the plane problem of elasticity. While the physical meaning of force is clear, the concept of dislocation may not be familiar to the reader and thus warrants an explanation. Although dislocations were not experimentally observed in materials until the 1950's, the concept of the dislocation was introduced and developed in elasticity theory by Volterra and Timpe in the early 1900's.

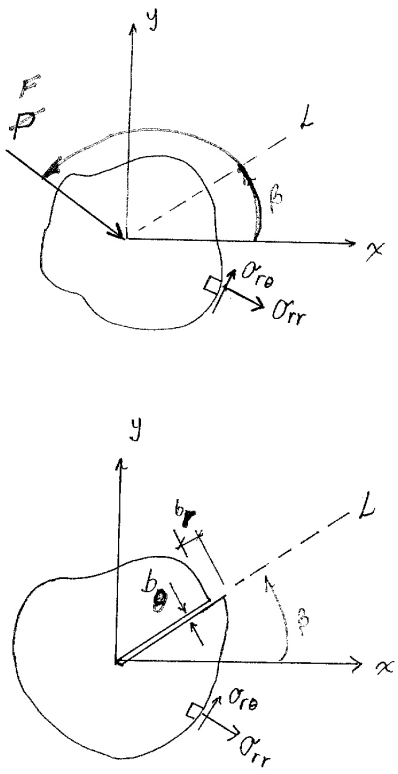

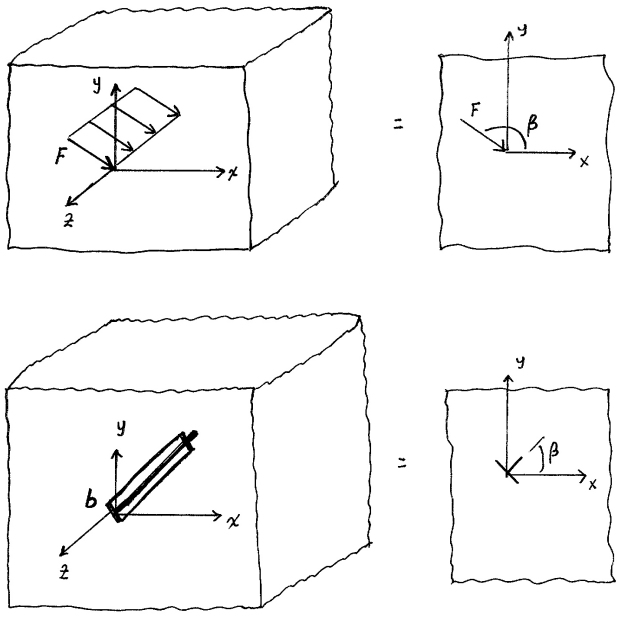

Fig. 3 Point force and dislocation representations

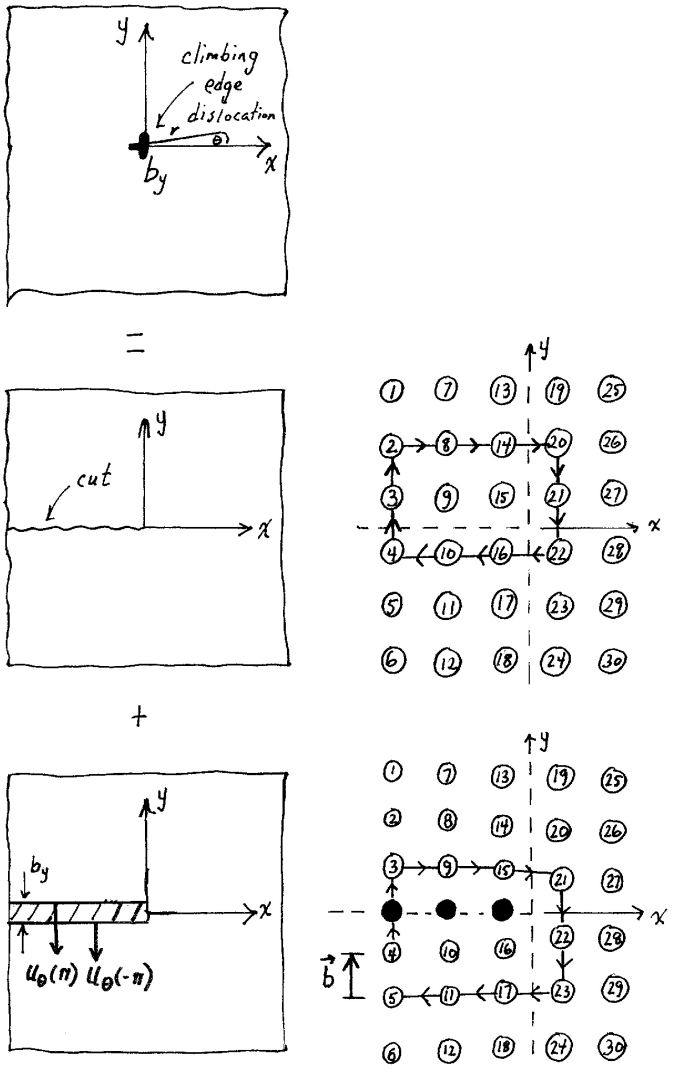

Fig. 4 Climbing edge dislocation

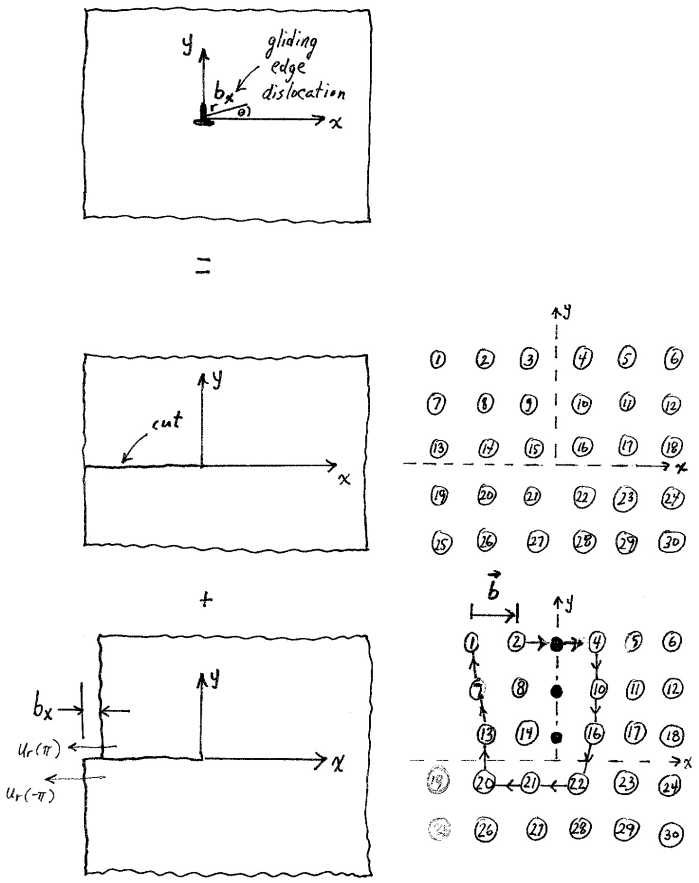

Fig. 5 Gliding edge disclocation

Consider first the so called ***climbing*** edge dislocation shown in Figure 4a. This configuration, which corresponds to $\beta = \pi$ in Figure 3, denotes the procedure shown in Figures 4b and 4d. A semi-infinite cut, defined as the ***slip plane***, is made along the negative $x-$axis. The slip plane terminates at the $z-$axis, which is defined as the ***dislocation line***. The upper and lower surfaces of this cut are displaced relative to each other in the $y-$direction by a distance b_y, and a rigid plate is inserted and welded to these surfaces. The typical crystallographic interpretation of this procedure is included in

In the previous lecture we derived the stress, strain and displacement fields in the immediate vicinity of a crack front in 3-D (crack tip in 2-D).

We then introduced the concepts of edge dislocation and point force. How will we use these solutions? The answer is that they provide features in their displacement and stress fields that will allow us to satisfy the boundary conditions of the problem by replacing them with their associated distributions and using superposition.

Let's have a preview of the method:

Previews

1. Use of point force

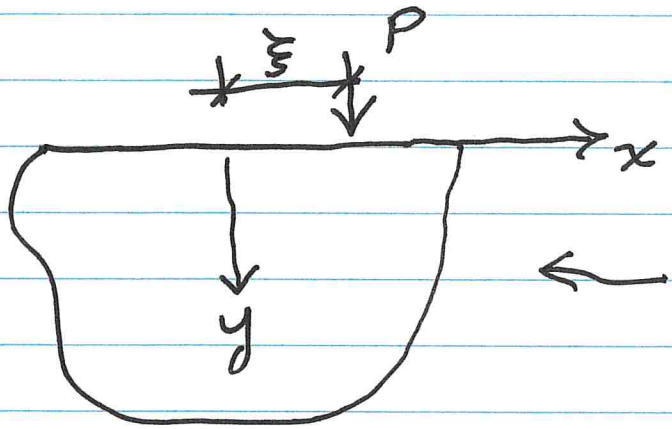

← this is the Flamant problem. We will solve it.

Consider the external crack:

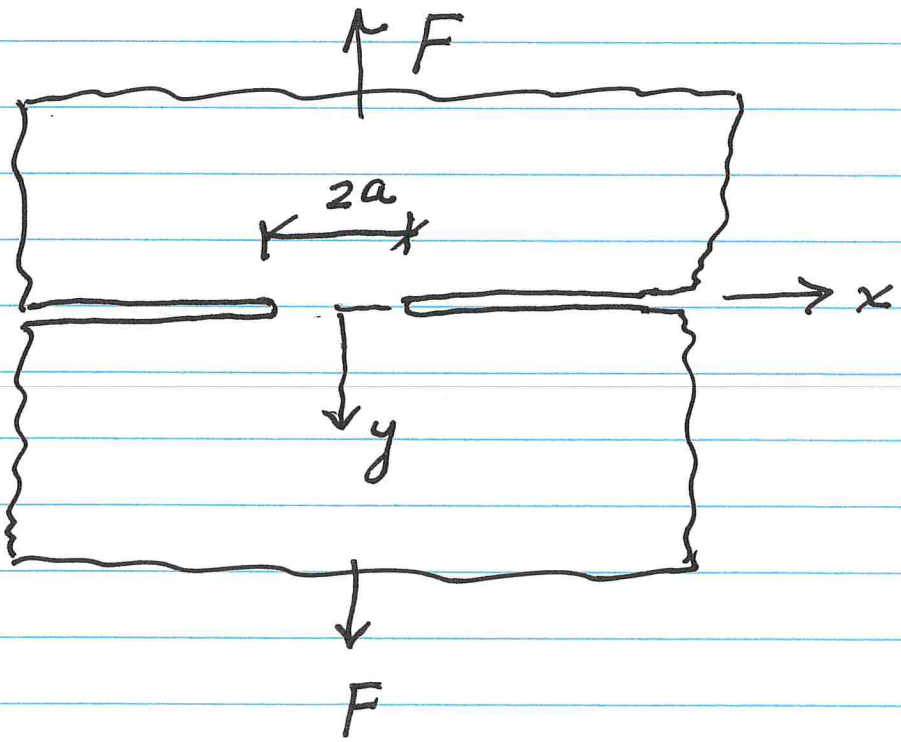

along $y=0$ $\sigma_{xy} = \frac{\partial u_y}{\partial x} = 0$ $-a < x < a$

$\sigma_{xy} = \sigma_{yy} = 0$ $|x| > a$

Free body diagram

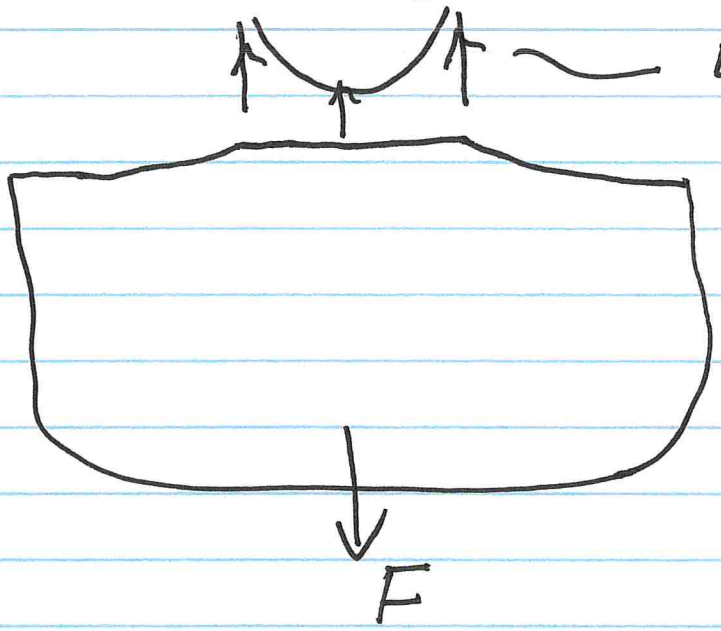

The problem is reduced to finding the $\sigma_{yy}(x)$ which provides

$$\frac{\partial u_y}{\partial x} = 0 \quad \text{and} \quad \int_{-a}^{a} \sigma_{yy}(x)\,dx = F$$

↑ uniqueness

Start with

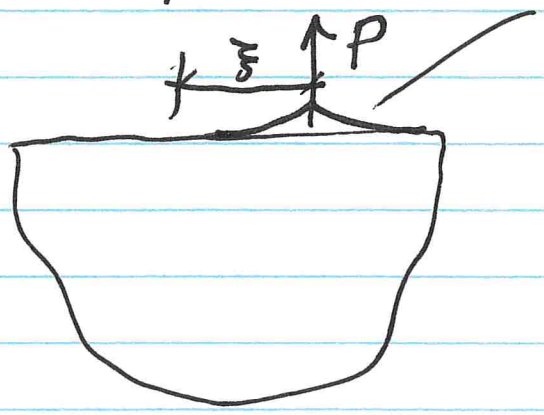

Single force does not satisfy $\frac{\partial u_y}{\partial x} = 0$

The "idea"

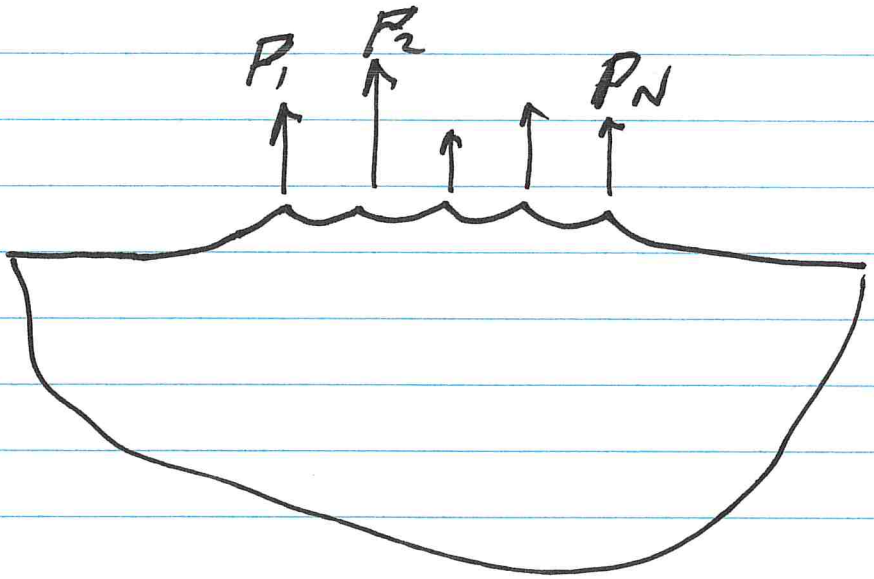

$P \longrightarrow \sigma_{yy}(x)dx$ (distribution)

in the limit the shape becomes the required straigh line.

2. Edge Dislocation:

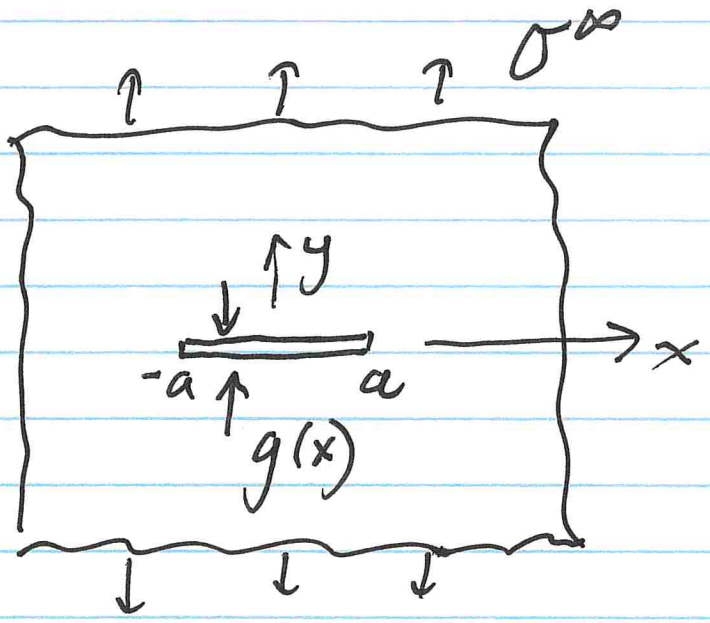

along $y=0$ $\quad \sigma_{xy} = \sigma_{yy} = 0 \quad |x| < a$

$\sigma_{xy} = 0 \quad |x| > a$

unknown is C.O.D. $\equiv g(x)$

The crack is a discontinuity of displacements! The source is therefore the edge dislocation!

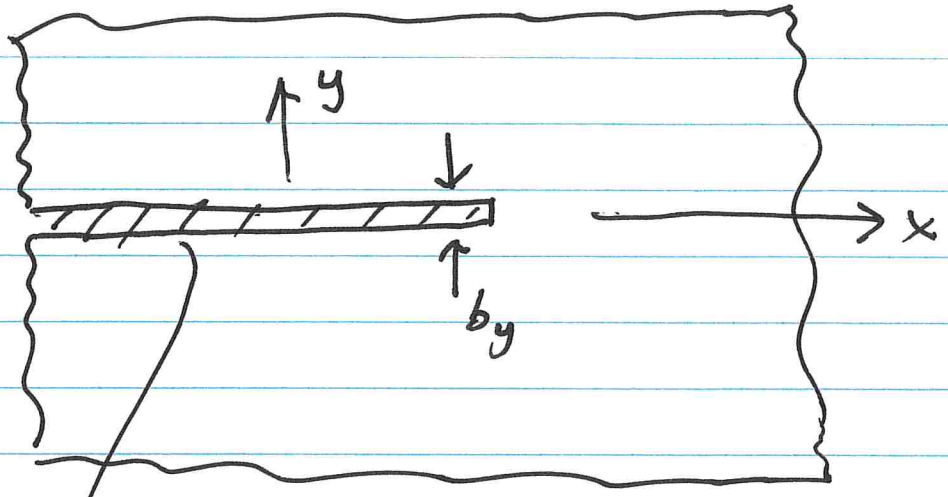

we will show $\sigma_{yy} \neq 0$

Let $b_y \equiv B(\xi)\,d\xi$

↳ distribution of dislocations

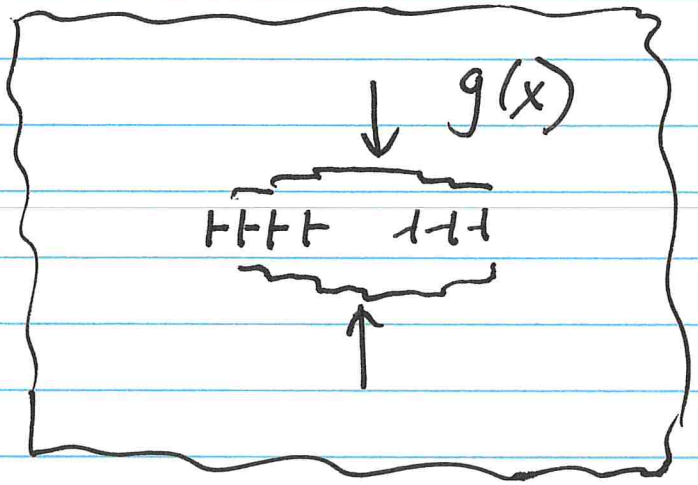

choose $B(\xi)$ which provides

$\sigma_{yy} = 0 \quad |x| < a$

Figures 4c and 4e, which represent lattice models of the elastic continuum. Figure 4c shows a perfect lattice consisting of 30 numbered atoms which comprise the neighborhood of the dislocation line. A circuit starting out at atom 4 comprised of ten consecutive steps, two in the positive $y-$direction, three in the positive $x-$direction, two in the negative $y-$direction, and finally three in the negative $x-$direction, leads back to atom 4. Figure 4e shows the configuration that results when an extra ***horizontal*** sheet of atoms is inserted between atom pairs 3-4, 9-10, and 15-16. Starting out at atom 4 and repeating the number, direction, and order of steps as in Figure 4c, this time crossing the slip plane, leads to atom 5. The ***Burgers*** vector $\vec{b}$, shown in Figure 4e, represents the vector perpendicular to the slip plane that is required to close the gap produced by the extra sheet. For this configuration the magnitude of the Burgers vector is b_y, and its direction is ***parallel*** to the dislocation line. Define the range of the polar angle as $-\pi < \theta \le \pi$. Then the Burgers vector introduces, as shown in Figure 4d, a discontinuous ***tangential*** displacement component along the negative $x-$axis, given by $u_\theta(-\pi) - u_\theta(\pi) = b_y$.

The ***gliding*** edge dislocation b_x is shown in Figure 5. For this case after the cut is made, the upper and lower surfaces are displaced relative to each other in the $x-$direction by a distance b_x, and then welded. The physical interpretation for this case is shown in Figures 5c and 5e. The row of atoms 1-7-13 are displaced relative to row 19-25 by a distance b_x in the positive $x-$direction. This procedure renders row 3-9-15 an extra half plane of atoms inserted between rows 2-8-14 and 4-10-16. Any circuit starting at atom 2 that crosses the slip plane ends up at atom 1, and the Burgers vector, which is ***perpendicular*** to the dislocation line, has a component in the $x-$direction whose

magnitude is b_x. For this configuration the ***radial*** displacement component along the negative $x-$axis is, for $-\pi < \theta \le \pi$, given by $u_r(-\pi) - u_r(\pi) = b_x$.

Note the similarity between the gliding and climbing edge dislocations. If atoms 19 and 25 are removed in Figure 52 and the sketch is rotated by 90 degrees counter clockwise, the climbing edge dislocation is recovered, atoms 3, 9 and 15 representing the extra sheet. In other words, for a fixed coordinate system, the only difference between the climbing edge dislocation and the gliding edge dislocation is the orientation of the extra half-plane, the first being inserted horizontally, the latter vertically. If the medium contains a *mixed* dislocation at a point, then the magnitude of the Burgers vector is given by $b = \sqrt{b_x^2 + b_y^2}$.

Derivation of the form of the stress fields

The stress, strain, and displacement fields associated with the point force and dislocation are derived next. Most books on dislocations that derive the solution to the edge dislocation problems reproduce the analysis based on Michell's general representation of the Airy stress function. The derivation presented here for both the edge dislocation and concentrated force problems relies on linearity and dimensional analysis to determine the ***form*** of the stress fields. The only relevant parameters in these elasticity problems besides the magnitude of the action (P or b) are r, θ, ν and E. Since the problems are linear the stress is proportional to the magnitude of the action

$$\sigma_{ij}^F \propto F \tag{18a}$$

$$\sigma_{ij}^b \propto b \tag{18b}$$

where the superscripts "b" and "F" are labels for the fields associated with the dislocation and point force, respectively. For the force the units of stress result by simply dividing Equation (18a) by r. For the dislocation, on the other hand, only E can provide units of stress. Multiplying Equation (18b) by E leads to dimensional inconsistency, which can be remedied by dividing the resulting equation by the only remaining available length parameter r. Consequently

$$\sigma_{ij}^{F} = \frac{F}{r} g_{ij}(\theta, \nu) \tag{19a}$$

$$\sigma_{ij}^{b} = \frac{b}{r} E f_{ij}(\theta, \nu) \tag{19b}$$

This argument has essentially provided the $r-$dependence of the stress fields, and has reduced the problem to the determination of functions f_{ij} and g_{ij}. Note that both stress fields possess a $\frac{1}{r}$ singularity. By absorbing the numerators of Equations (19) into common functions A_{ij}, which may depend on θ, E, ν, b, F, ***but not on*** r, the solutions to both problems can be expressed as

$$\sigma_{ij}^{b,F} \equiv \sigma_{ij} = \frac{A_{ij}(\theta)}{r} \tag{20}$$

The distinction between the point force and dislocation is made by requiring different force and displacement jump conditions on a contour surrounding their point of application. The force, as shown in Figure 6a, is equilibriated by the tractions acting on

any closed contour surrounding its point of application. Moreover, the displacements are continuous across any line L. For the dislocation, as shown in Figure 6b, the tractions are self-equilibriated, and the magnitudes of the radial and tangential displacement discontinuities across the slip plane L are equal to b_r and b_θ.

Equilibrium and compatibility provide three equations for the three unknown A_{ij}

$$\frac{\partial \sigma_{rr}}{\partial r} + \frac{\sigma_{rr} - \sigma_{\theta\theta}}{r} + \frac{1}{r}\frac{\partial \sigma_{r\theta}}{\partial \theta} = 0 \tag{21a}$$

$$\frac{1}{r}\frac{\partial \sigma_{\theta\theta}}{\partial \theta} + 2\frac{\sigma_{r\theta}}{r} + \frac{\partial \sigma_{r\theta}}{\partial r} = 0 \tag{21b}$$

$$\left(\frac{\partial^2}{\partial r^2} + \frac{1}{r}\frac{\partial}{\partial r} + \frac{1}{r^2}\frac{\partial^2}{\partial \theta^2}\right)\left(\sigma_{rr} + \sigma_{\theta\theta}\right) = 0 \tag{21c}$$

With Equations (20), Equations (21) are transformed into the ordinary differential equations

$$-A_{\theta\theta} + \frac{dA_{r\theta}}{d\theta} = 0 \tag{22a}$$

$$A_{r\theta} + \frac{dA_{\theta\theta}}{d\theta} = 0 \tag{22b}$$

$$A_{rr} + A_{\theta\theta} + \frac{d^2}{d\theta^2}\left(A_{rr} + A_{\theta\theta}\right) = 0 \tag{22c}$$

The solution of the last equation is

$$A_{rr} + A_{\theta\theta} = c_3 \cos\theta + c_4 \sin\theta \tag{23}$$

Differentiating Equation (22a) and adding the result to Equation (22b) leads to

$$\frac{d^2 A_{r\theta}}{d\theta^2} + A_{r\theta} = 0 \tag{24}$$

whose solution, together with Equations (22a) and (23), provides

$$A_{r\theta} = c_1 \cos\theta + c_2 \sin\theta \tag{25a}$$

$$A_{\theta\theta} = -c_1 \sin\theta + c_2 \cos\theta \tag{25b}$$

$$A_{rr} = \left(c_3 - c_2\right)\cos\theta + \left(c_4 + c_1\right)\sin\theta \tag{25c}$$

The unknown constants c_1, c_2, c_3, c_4 for the force and for the dislocation are determined next using the previously discussed force and displacement jump conditions.

The (Symmetric Problem)

Without loss of generality the solution is developed to the problem which is "symmetric" with respect to the $x-$axis, which corresponds to $\beta = \pi$ in Figures 3 and 6. That is, the physics is invariant to a reflection about the *x*-axis The word symmetric is in quotes because while certain physical quantities are symmetric about the $x-$axis, others are asymmetric. The ***positive*** stress and displacement components at $\pm\theta$ are shown in solid arrows in Figure 7. The dashed arrows indicate the ***required*** directions of $\sigma_{r\theta}$ and u_θ for the picture to be symmetric about the $x-$axis. This symmetry requires

$$\sigma_{rr}(+\theta) = \sigma_{rr}(-\theta) \tag{26a}$$

$$\sigma_{\theta\theta}(+\theta) = \sigma_{\theta\theta}(-\theta) \tag{26b}$$

$$\sigma_{r\theta}(+\theta) = -\sigma_{r\theta}(-\theta) \tag{26c}$$

$$u_r(+\theta) = u_r(-\theta) \tag{26d}$$

$$u_\theta(+\theta) = -u_\theta(-\theta) \tag{26e}$$

which make $c_1 = c_4 = 0$.

Consider a circular free body diagram of unit radius surrounding the point of action, as shown in Figure 6a. For $\beta = \pi$, the net force per unit thickness resulting from the tractions along the circular boundary satisfies the equilibrium equations

$$\int_{-\pi}^{\pi}\left(\sigma_{rr}\cos\theta - \sigma_{r\theta}\sin\theta\right)r d\theta = P_x + \int_{-\pi}^{\pi}\left(A_{rr}\cos\theta - A_{r\theta}\sin\theta\right)d\theta = \begin{cases} -F_x & \text{for the force} \\ 0 & \text{for the dislocation} \end{cases} \tag{27}$$

By substituting Equation (25a) and Equation (25c) into Equation (27) if follows that

$$\pi(c_2 - c_5) = \begin{cases} F_x & \text{for the force} \\ 0 & \text{for the dislocation} \end{cases} \tag{28}$$

Equation (28) provides the first relation between the unknown constants c_2 and $c_5 \equiv c_3 - c_2$. The second equation, which specifies the displacement discontinuity,

requires the calculation of the displacements, which can be determined through the strain-displacement relations and Hooke's Law

$$\varepsilon_{rr} = \frac{\partial u_r}{\partial r} = \frac{1}{2\mu}\left[\sigma_{rr} - \frac{(3-\kappa)}{4}(\sigma_{rr} + \sigma_{\theta\theta})\right] \tag{29a}$$

$$\varepsilon_{\theta\theta} = \frac{1}{r}\left(\frac{\partial u_\theta}{\partial \theta} + u_r\right) = \frac{1}{2\mu}\left[\sigma_{\theta\theta} - \frac{(3-\kappa)}{4}(\sigma_{rr} + \sigma_{\theta\theta})\right] \tag{29b}$$

$$\varepsilon_{r\theta} = \frac{1}{2}\left(\frac{1}{r}\frac{\partial u_r}{\partial \theta} + \frac{\partial u_\theta}{\partial r} - \frac{u_\theta}{r}\right) = \frac{1}{2\mu}\sigma_{r\theta} \tag{29c}$$

Integrating ε_{rr} and $\varepsilon_{\theta\theta}$

$$u_r = \frac{1}{2\mu}\cos\theta \ln r\left[c_5 - \frac{(3-\kappa)}{4}(c_2 + c_5)\right] + \frac{df(\theta)}{d\theta} \tag{30a}$$

$$u_\theta = \frac{1}{2\mu}\sin\theta\left\{c_2 - \frac{(3-\kappa)}{4}(c_2 + c_5) - \ln r\left[c_5 - \frac{(3-\kappa)}{4}(c_2 + c_5)\right]\right\} - f(\theta) + g(r) \tag{30b}$$

where the functions of integration f, g are determined through the equation that results from substitution of Equations (30) into Equation (29c)

$$\frac{d^2 f}{d\theta^2} + f - \frac{1}{2\mu}\sin\theta\left[2c_2 + \left(\frac{c_2 + c_5}{2}\right)(\kappa - 1)\right] = g - r\frac{dg}{dr} \tag{31}$$

The left hand side of Equation (31) is a function of θ, while the right hand side is a function of r. Therefore both sides are equal to a constant k. Solving the right hand side of Equation (31) we obtain

$$g(r) = k + \omega r \tag{32}$$

The contribution from g to u_θ and u_r represents, as discussed previously, a rigid body translation and rigid body rotation. Setting $k = \omega = 0$, the general solution for f is the addition of the homogeneous and particular solutions

$$f = c_6 \sin\theta + c_7 \cos\theta + \theta\left(c_8 \sin\theta + c_9 \cos\theta\right) \tag{33}$$

where the homogeneous solution $c_6 \sin\theta + c_7 \cos\theta$ represents a rigid body translation that is also set equal to zero. Substitution of Equation (33) into Equation (31) provides $c_8 = 0$ and $c_9 = -\frac{1}{4\mu}\left[2c_2 + \left(\frac{c_2 + c_5}{2}\right)(\kappa - 1)\right]$. The final expressions for the displacements components become

$$u_r = \frac{1}{2\mu}\cos\theta \ln r\left[c_5 - \frac{(3-\kappa)}{4}(c_2 + c_5)\right] + \frac{1}{4\mu}\left[2c_2 + \left(\frac{c_2 + c_5}{2}\right)(\kappa - 1)\right](\theta\sin\theta - \cos\theta) \tag{34a}$$

$$u_\theta = \frac{1}{2\mu}\sin\theta\left\{c_2 - \frac{(3-\kappa)}{4}(c_2 + c_5) - \ln r\left[c_5 - \frac{(3-\kappa)}{4}(c_2 + c_5)\right]\right\} + \frac{1}{4\mu}\left[2c_2 + \left(\frac{c_2 + c_5}{2}\right)(\kappa - 1)\right]\theta\cos\theta \tag{34b}$$

As expected, the displacement solutions include multivalued functions, namely $\theta\sin\theta$ and $\theta\cos\theta$. As mentioned previously, the slip plane can be placed along $\beta=\pi$ by placing the *branch cut* along the negative $x-$axis, that is, defining the range $-\pi<\theta\le\pi$. If it is desired to place the slip plane along $\beta=0$, then the polar angle should be defined in the range $0\le 0<\pi$. Both choices lead to a continuous radial displacement component, i.e., $u_r(\pi)-u_r(-\pi)=u_r(0)-u_r(2\pi)=0$, and a discontinuous tangential component given, for the respective definitions of the polar angle, by

$$u_\theta(\pi)-u_\theta(-\pi)=u_\theta(0)-u_\theta(\pi)=-\frac{\pi}{4\mu}\left[2c_2+\left(\frac{c_2+c_5}{2}\right)(\kappa-1)\right]=\begin{cases}0 & \text{for the force}\\ b_y & \text{for the dislocation}\end{cases} \tag{35}$$

For the dislocation with slip plane placed along the negative *x*-axis (the gap between the upper (+) and lower (-) surfaces is given by $g(x)\equiv u_y^+(x)-u_y^-(x)=-u_\theta(\pi)+u_\theta(-\pi)=b_y$), Equations (27) and (35) provide

$$c_2=c_5=\frac{2\mu b_y}{\pi(\kappa+1)} \tag{36a}$$

$$\sigma_{rr}=\sigma_{\theta\theta}=\frac{2\mu b_y}{\pi(\kappa+1)}\frac{\cos\theta}{r} \tag{36b}$$

$$\sigma_{r\theta}=\frac{2\mu b_y}{\pi(\kappa+1)}\frac{\sin\theta}{r} \tag{36c}$$

$$u_\theta = \frac{b_y}{2\pi(\kappa+1)}\left[(\kappa+1)\theta\cos\theta-(\kappa-1)\sin\theta\ln r-\sin\theta\right]+\frac{b_y}{2\pi(\kappa+1)}\kappa\sin\theta \qquad (36d)$$

$$u_r = \frac{b_y}{2\pi(\kappa+1)}\left[(\kappa+1)\theta\sin\theta+(\kappa-1)\cos\theta\ln r-\cos\theta\right]-\frac{b_y}{2\pi(\kappa+1)}\kappa\sin\theta \qquad (36e)$$

The last term in each of Equations (36d) and (36e) represents a rigid body translation, and can be omitted. As expected, the hoop stress along the positive $x-$axis is tensile.

If the slip plane is desired along the positive $x-$axis, then the displacement discontinuity should be prescribed as $u_\theta(0)-u_\theta(2\pi)=b_y$. This choice will lead to stress and displacement components equal to the negative of those given by Equations (36), and as expected, positive hoop stress along the negative $x-$axis.

For the point force we find

$$c_2 = \frac{(\kappa-1)}{2\pi(\kappa+1)}F \qquad c_5 = -\frac{(\kappa+3)}{2\pi(\kappa+1)}F \qquad (37a)$$

$$\sigma_{rr} = -\frac{(\kappa+3)F}{2\pi(\kappa+1)}\frac{\cos\theta}{r} \qquad (37b)$$

$$\sigma_{\theta\theta} = \frac{(\kappa-1)F}{2\pi(\kappa+1)}\frac{\cos\theta}{r} \qquad (37c)$$

$$\sigma_{r\theta} = \frac{(\kappa-1)F}{2\pi(\kappa+1)}\frac{\sin\theta}{r} \qquad (37d)$$

$$u_\theta = \frac{F}{2\pi\mu(\kappa+1)}\left[\kappa\sin\theta\ln r+\sin\theta\right] \qquad (37e)$$

$$u_r = \frac{F}{2\pi\mu(\kappa+1)}\left[-\kappa\cos\theta\ln r\right] \qquad (37f)$$

Plots of the stress components produced by the dislocation and point force are shown in Figures 8 and 9.

Exercise 1

Derive expressions for the components of stress and displacement associated with a concentrated force applied at the surface of a half-plane, as shown in the figure.

Solution:

$$\sigma_{rr} = -\frac{2P}{\pi}\frac{\cos\theta}{r}$$

$$\sigma_{r\theta} = \sigma_{\theta\theta} = 0$$

$$u_\theta = -\frac{P}{4\pi\mu}\left[(\kappa-1)\theta\cos\theta - (\kappa+1)\sin\theta\ln r - \sin\theta\right]$$

$$u_r = -\frac{P}{4\pi\mu}\left[(\kappa-1)\theta\sin\theta + (\kappa+1)\cos\theta\ln r - \cos\theta\right]$$

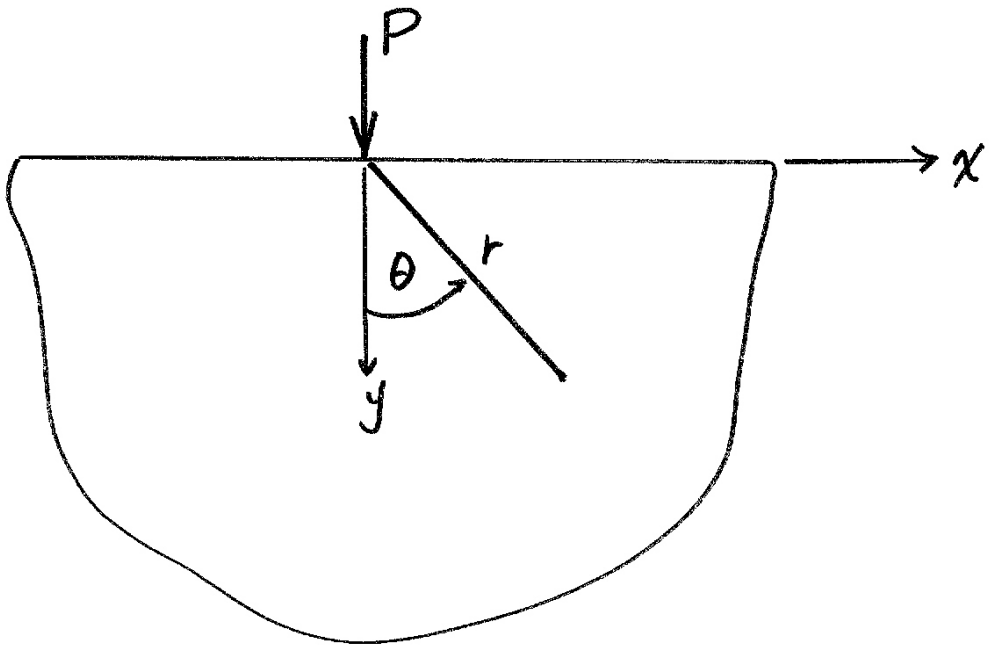

Exercise 2

Derive expressions for the stress and displacement fields produced by a gliding edge dislocation.

THE USE OF FUNDAMENTAL SINGULAR SOLUTIONS OF ELASTICITY TO SOLVE CRACK PROBLEMS

This chapter presents several examples that illustrate how the previously derived discrete dislocation and point force solutions can be used to formulate the solutions of *plane* boundary value problems involving cracks. The approach involves the use of distributed dislocations and forces, and is referred to as the *Green's function method*, reduces elasticity problems to a system of one dimensional *singular integral equations*. A brief description of how the method can be used to formulate three dimensional problems is provided in the Appendix.

Many mathematical techniques are available to solve the field equations of elasticity. The Green's function method is presented in this book because the approach and the resulting equations have a clear physical interpretation. The discussion also emphasizes that even for relatively simple configurations, sophisticated mathematics is needed to derive explicit solutions for crack opening displacements and stress intensity factors. The method relies on the knowledge of a fundamental solution that satisfies as many of the boundary conditions of the problem, and provides the necessary force or displacement discontinuity. Replacing the concentrated action with a continuous distribution enables one to write the remaining boundary conditions as a system of integral equations.

Paramount to the development of solutions using the Green's function method is the understanding of boundary and symmetry conditions. As will be shown through several examples, this understanding guides the formulation of a physically motivated superposition scheme.

Example: The Exterior Crack

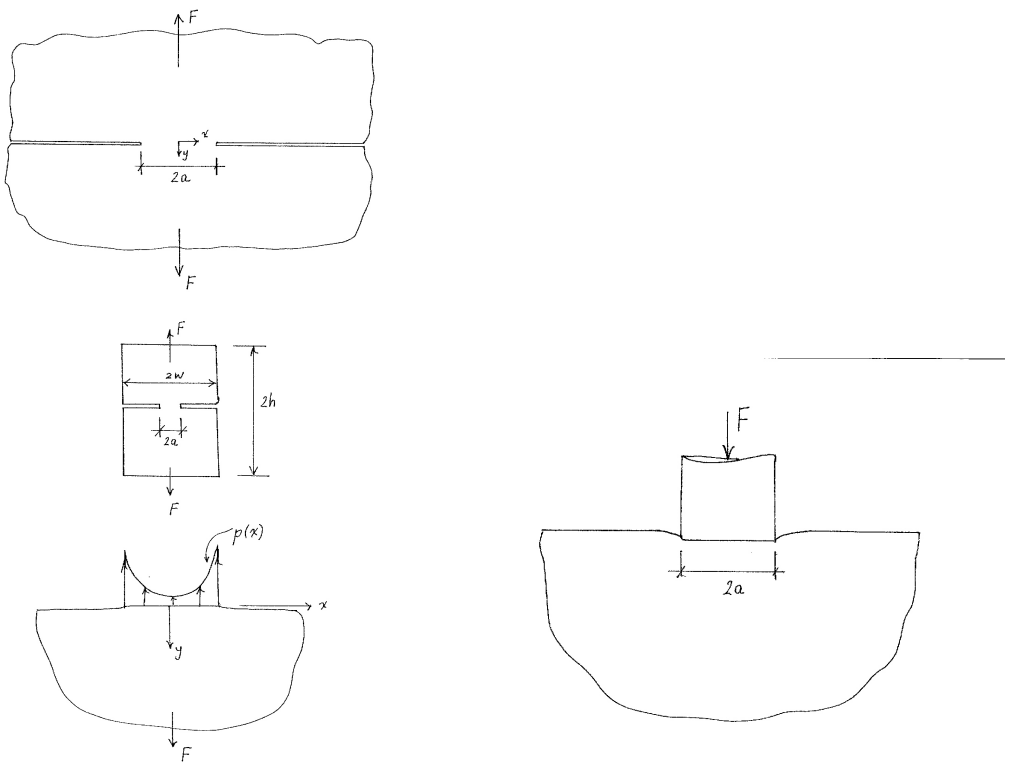

Fig. 3.1 The exterior crack problem

The *exterior* crack shown in Figure 3.1a is perhaps the simplest crack problem that can be used to demonstrate the Green's function method. An infinitely extended plate containing two semi-infinite cracks whose tips are separated by an uncracked ligament of length $2a$ is loaded by two concentrated forces F at infinity. This configuration corresponds to the deeply cracked limiting case $\frac{a}{W}, \frac{a}{h} << 1$ of the finite geometry problem shown in Figure 3.1b. For this configuration the $x-$axis is a line of symmetry. The boundary conditions are

$$\sigma_{yy} = \sigma_{xy} = 0 \qquad y = 0 \qquad |x| > a$$

(3.1a)

$$\sigma_{xy} = 0 \qquad y = 0 \qquad |x| < a$$

(3.1b)

$$\frac{\partial u_y}{\partial x} = 0 \qquad y = 0 \qquad |x| < a$$

(3.1c)

Equation (3.1a) represents the zero traction boundary condition along the crack surfaces, while Equations (3.1b) and (3.1c) follow from the requirement that all points lying along the line of symmetry have zero shear stress and equal values of displacement in the $y-$direction. The use of the derivative of the displacement in Equation (3.1c) eliminates the rigid body displacement from the elasticity problem.

The boundary conditions suggest that this problem is equivalent to the problem of a half-plane subjected to an *unknown* surface stress distribution $p(x)$ shown in Figure 3.1c, that represents the stress transferred across the uncracked ligament. Equations (3.1a) and (3.1b) are automatically satisfied, and $p(x)$ is required to produce a displacement profile that satisfies Equation (3.1c). As such, the exterior crack problem is equivalent, except for the sign of the stress distribution, to the problem of a rigid flat dye coming into frictionless contact with an elastic half-plane, as shown in Figure 3.1d.

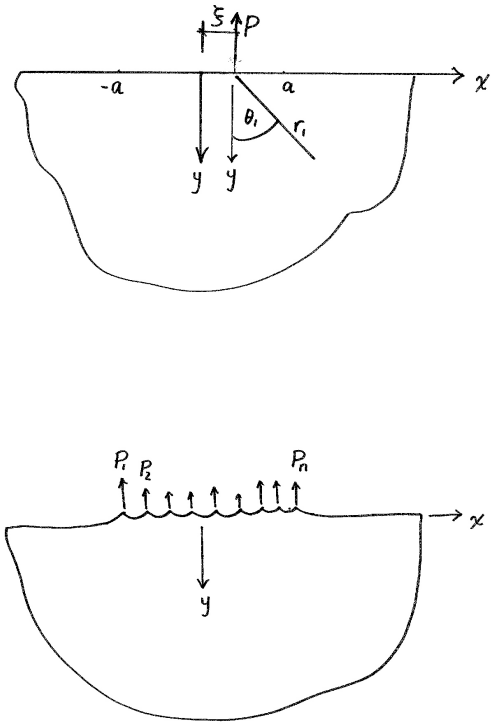

Fig. 3.2

The Green's function approach to this problem relies on the fundamental solution of the problem shown in Figure 3.2a. The concentrated force acting at point $x = \xi$ produces a displacement profile on the surface of the half-plane which, as shown next, does not satisfy Equation (3.1c). However, one can envision, as shown in Figure 3.2b, that a properly selected distribution of concentrated forces can produce, in the limit of infinite number of forces, the desired displacement profile. This limit corresponds to a continuous force distribution $p(\xi)$, that produces, in the interval $d\xi$, a net force $dP = p(\xi)d\xi$. The function $\frac{\partial u_y}{\partial x}$ along $y = 0$ produced by the concentratred force can be calculated from the analytic solution for the displacements of this problem that were derived in Exercise 1 of Chapter 1

$$u_{\theta_1} = -\frac{P}{4\pi\mu}\left[(\kappa-1)\theta_1\cos\theta_1 - (\kappa+1)\sin\theta_1\ln r_1 - \sin\theta_1\right]$$

(3.2)

where $r_1 = \sqrt{(x-\xi)^2 + y^2}$ and $\theta_1 = \tan^{-1}\left(\frac{x-\xi}{y}\right)$.

On the surface, $\theta_1 = \frac{\pi}{2}$

$$u_{\theta 1}\left(\frac{\pi}{2}\right) = -u_y(y=0) = \frac{P}{4\pi\mu}\left[(\kappa+1)\ln r_1 + 1\right]$$

(3.3)

Differentiation of Equation (3.3) yields

$$\frac{\partial u_y}{\partial x} = -\frac{(\kappa+1)}{4\pi\mu}\frac{P}{(x-\xi)} \qquad y = 0$$

(3.4)

which, as mentioned previously, does not satisfy boundary condition (3.1c). Replacing the concentrated force in Equation (3.4) with the continuous distribution defined within the interval (*-a,a*), and integrating the effect of each force embedded in the distribution, enables boundary condition (3.1c) to be written as the *singular integral equation*

$$\frac{\partial u_y}{\partial x} = -\frac{(\kappa+1)}{4\pi\mu}\int_{-a}^{a}\frac{p(\xi)d\xi}{(x-\xi)} = 0 \qquad y = 0 \quad |x| < a$$

(3.5)

Equation (3.5) is referred to as an integral equation because the unknown function $p(\xi)$ appears under the integral sign. Because the unknown function appears only under

the integral sign, the equation is defined as being of the *first kind*. If the unknown function in an integral equation appears inside and ouside the integral sign, the integral equation is defined as being of the *second kind*. Equations of the second kind appear in the solution of interface crack problems and certain contact problems involving friction. Equation (3.5) illustrates the difference between the integral equation and the differential equation formulations of the boundary value problem. Differential equations are *subjected* to boundary conditions, while integral equations *are* boundary conditions. In this problem the integral equation represents the displacement boundary condition along the uncracked ligament.

Equation (3.5) does not have a unique solution because, as will be shown during the solution process, there are an infinite number of force distributions $p(\xi)$ that satisfy this equation, each corresponding to a different value of the total load. A unique solution is obtained by requiring the distribution to be in equilibrium with the applied force F

$$F + \int_{-a}^{a} p(\xi) d\xi = 0$$

(3.6)

The problem is therefore reduced to the determination of the stress distribution $p(\xi)$ that satisfies Equations (3.5) and (3.6).

Aside: Solution of Singular Integral Equations

The solution of the equation

$$\int_{-1}^{1} \frac{\varphi(\xi) d\xi}{(\xi - x)} = f(x) \qquad -1 < x < 1$$

(3.7)

is given by

$$\varphi(x) = -\frac{1}{\pi^2} w(x) \int_{-1}^{1} \frac{f(\xi) d\xi}{w(\xi)(\xi - x)} + C w(x)$$

(3.8)

The characteristic function $w(x)$ and the constant C, which depend on the nature of the singularity at the endpoints $x = \pm 1$, are listed in Table 3.1. Equation (3.7) and the integrals listed in Table 3.2 can be derived using complex variable techniques that are beyond the scope of this book. The reader interested in the derivation is referred to Muskhelishvili's books.

Nature of Singularity	$w(x)$	C
Bounded at $x = \pm 1$	$\sqrt{1 - x^2}$	0
Singular at $x = -1$, bounded at $x = +1$	$\sqrt{\frac{1 - x}{1 + x}}$	0
Singular at $x = +1$, bounded at $x = -1$	$\sqrt{\frac{1 + x}{1 - x}}$	0
Singular at $x = \pm 1$	$\frac{1}{\sqrt{1 - x^2}}$	to be determined as part of the solution

Table 3.1 Characteristic Functions for Singular Integral Equation of the First Kind

Solutions that are bounded at both endpoints satisfy the consistency condition

$$\int_{-1}^{1} \frac{f(\xi)d\xi}{w(\xi)} = 0$$

(3.9)

Some useful integrals that appear often in the solution of singular integral equations of the first kind, are tabulated in Table 3.2.

Table 3.2 Integral Formulas

Integral	$-1 < x < 1$	$\lvert x \rvert > 1$
$\int_{-1}^{1} \frac{d\xi}{(\xi - x)\sqrt{1-\xi^2}}$	0	$\pm \frac{\pi}{\sqrt{x^2-1}}$
$\int_{-1}^{1} \frac{\xi d\xi}{(\xi - x)\sqrt{1-\xi^2}}$	π	$\pi \pm \frac{\pi x}{\sqrt{x^2-1}}$
$\int_{-1}^{1} \frac{\xi^2 d\xi}{(\xi - x)\sqrt{1-\xi^2}}$	πx	$x\left(\pi \pm \frac{\pi x}{\sqrt{x^2-1}}\right)$

In Table 3.2 the $+(-)$ sign in the third column corresponds to $x < -1$ $(x > 1)$.

By making the substitutions $t \equiv \frac{\xi}{a}$, $s \equiv \frac{x}{a}$ and $\hat{p}(t) \equiv \frac{a}{F} p(t)$, Equations (3.5) and (3.6) can be written in the form of Equation (3.7)

$$\int_{-1}^{1} \frac{\hat{p}(t)dt}{(s-t)} = 0 \qquad |s| < 1$$

(3.10a)

$$\int_{-1}^{1} \hat{p}(t)dt = -1$$

(3.10b)

Symmetry about the $y-$axis eliminates the possibility of a solution that is bounded at one end and singular at the other. Moreover, since the right hand side of

Equation (3.10a) is zero, the bounded solution $p(x) = 0$, which follows from Equation (3.8), does not satisfy Equation (3.10b)

The nonunique solution is therefore given by

$$\hat{p}(s) = \frac{C}{\sqrt{1-s^2}}$$

(3.11)

in terms of the arbitrary constant C. Uniqueness is achieved by enforcing the equilibrium Equation (3.6), which yields

$$\int_{-1}^{1} \hat{p}(\xi) d\xi = C\left(\sin^{-1}(1) - \sin^{-1}(-1)\right) = -1$$

(3.12)

so that $C = -\frac{1}{\pi}$. The solution for the stress across the ligament is therefore

$$\sigma_{yy} = -p(x) = \frac{F}{\pi\sqrt{a^2 - x^2}}$$

(3.13)

As expected, the stress is square root singular near the crack tips. The stress intensity factor is determined as

$$K_I \equiv \lim_{x \to a^-} \left[\sqrt{2\pi(a-x)}\sigma_{yy}\right] = \lim_{x \to a^-} \left[\sqrt{2\pi(a-x)}\frac{F}{\pi\sqrt{(a+x)(a-x)}}\right] = \frac{F}{\sqrt{\pi a}}$$

(3.14)

This solution agrees with the one reported in Tada's handbook.

Example: The Griffith Crack

Figure 3.3a shows the so called Griffith crack of length $2a$ loaded by a remote uniform tensile stress σ^{∞}. The boundary and symmetry conditions for this Mode-I configuration are

$$\sigma_{yy} = 0 \qquad y = 0 \qquad |x| < a$$

(3.15a)

$$\sigma_{xy} = 0 \qquad y = 0 \qquad |x| < a$$

(3.15b)

$$\sigma_{xy} = \frac{\partial u_y}{\partial x} = 0 \qquad y = 0 \qquad |x| > a$$

(3.15c)

$$\sigma_{yy} \to \sigma^{\infty} \text{ as } y \to \infty$$

(3.15d)

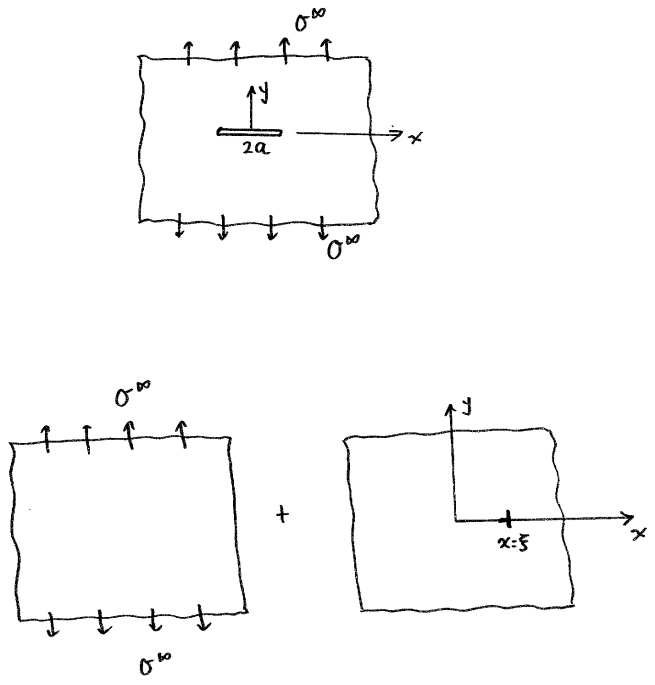

Fig. 3.3

The crack is a line across which the displacement component u_y is discontinuous. The unknown function in this problem is the crack opening displacement $g(x)$. This suggests the use of the dislocation Green's function, since it provides the necessary discontinuity in displacement. Consider the superposition of the stress and displacement fields produced by a uniform tensile stress and by a discrete dislocation placed at point $x = \xi$ (with slip plane to the *left* of $x = \xi$), as shown in Figure 3.3b. Denote the fields produced by the uniform stress and the discrete dislocation by superscripts ∞ and d, respectively. The uniformly stressed plane satisfies all Equations (3.15). It follows from Equation (1.36b) of Chapter 1 that the discrete dislocation satisfies Equations (3.15b) and (3.15c), but not (3.15a), since

$$\sigma_{xy}^{d} = u_{y}^{d} = 0 \qquad y = 0$$

(3.16a)

$$\sigma_{yy}^{d} = \frac{2\mu b_y}{\pi(\kappa+1)}\frac{1}{(x-\xi)} \qquad y=0$$

(3.16b)

Furthermore, since the slip plane is along the negative $x-$axis $(-\pi < \theta \le \pi)$ the discontinuity in displacement can be written in terms of the Heaviside function

$$H(t) \equiv \begin{cases} 0 & t<0 \\ 1 & t>0 \end{cases}$$

(3.17)

as

$$g^{d}(x) = b_y H(\xi - x)$$

(3.18)

The stress and displacement fields, obtained from the superposition of the uniform stress field and discrete dislocation, satisfy Equations (3.15b), (3.15c) and (3.15d). The total traction on $y=0$ is

$$\sigma_{yy} = \sigma_{yy}^{\infty} + \sigma_{yy}^{d} = \sigma_{yy}^{\infty} + \frac{2\mu b_y}{\pi(\kappa+1)}\frac{1}{(x-\xi)} \qquad y=0$$

(3.19)

Just as the point force did not satisfy the displacement boundary condition along the uncracked ligament in the exterior crack example, the discrete dislocation does not satisfy the traction boundary condition along the surfaces of the Griffith crack. The solution was developed for the exterior crack by replacing the concentrated force with a

distributed force. An analogous distribution for the dislocation is called the *dislocation density*, which follows from the ideas shown schematically in Figure 3.4.

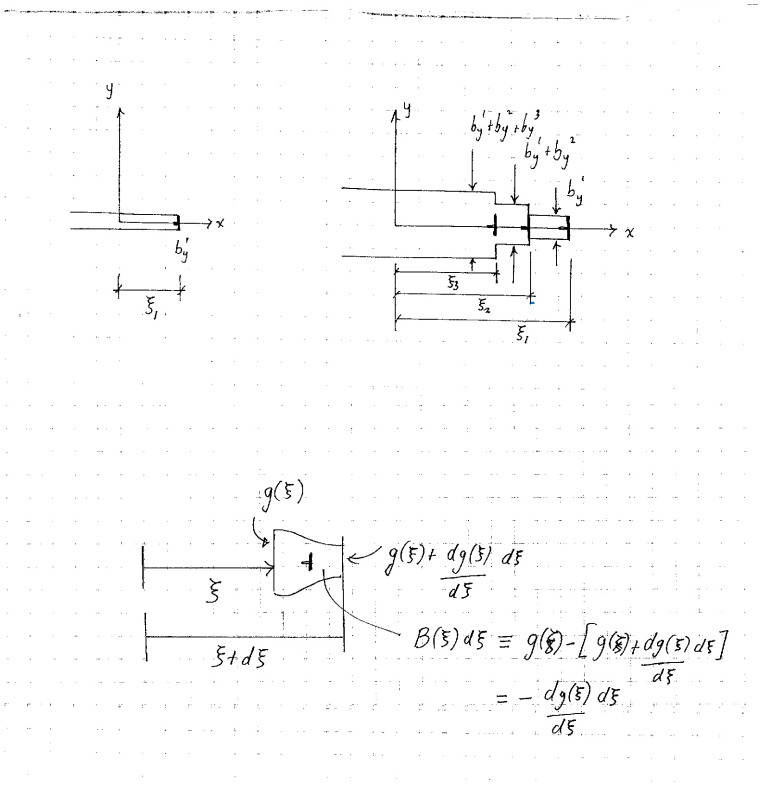

Fig. 3.4

As shown in Figure 3.4a, dislocation b_y^1 placed at $x=\xi_1$ produces a discontinuity to the left of the dislocation. If an additional dislocation of the same sign and magnitude b_y^2 is placed at $x=\xi_2$ the net effect is a discontinuity of magnitude $b_y^1+b_y^2$ to the left of point $x=\xi_2$, and a discontinuity of magnitude b_y^1 from $x=\xi_2$ to $x=\xi_1$. By selecting the position, magnitude, and sign of additional dislocations, this procedure can be used to create a staircase opening of any desired shape, as shown in Figure 3.4b. Analogous to

the distributed load, the dislocation distribution is defined in terms of its density $B(\xi)$ such that it produces, in the interval $d\xi$, a net Burgers vector $db = B(\xi)d\xi$. With respect to Figure 3.4c, db is equal to the difference in the gap between points ξ and $\xi + d\xi$,

$$-db = B(\xi)d\xi = \left[g(\xi) + \frac{dg(\xi)}{d\xi} d\xi \right] - g(\xi) = \frac{dg(\xi)}{d\xi} d\xi \qquad (3.20)$$

Equation (3.20) defines the dislocation density as

$$B(\xi) = \frac{dg(\xi)}{d\xi}$$

(3.21)

Replacing the discrete dislocation in Equations (3.18) and (3.19) with the dislocation density, and integrating the effects of each dislocation embedded in the distribution along the infinite interval yields

$$\sigma_{yy} = \sigma^{\infty} + \frac{2\mu}{\pi(\kappa+1)} \int_{-\infty}^{\infty} \frac{B(\xi)d\xi}{x-\xi} \qquad y = 0$$

(3.22a)

$$g(x) = \int_{-\infty}^{\infty} B(\xi)H(\xi - x)d\xi = \int_{-\infty}^{x} B(\xi)(0)d\xi + \int_{x}^{\infty} B(\xi)(1)d\xi = \int_{x}^{\infty} B(\xi)d\xi$$

(3.22b)

For the Griffith crack the dislocations are distributed along the interval $|x| < a$, along which Equation 3.16a demands that

$$\frac{2\mu}{\pi(\kappa+1)}\int_{-a}^{a}\frac{B(\xi)d\xi}{\xi-x}=\sigma^{\infty} \qquad y=0 \quad |x|<a$$

(3.23)

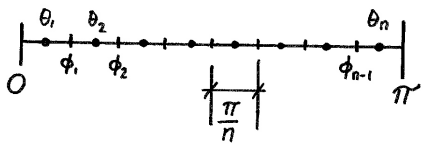

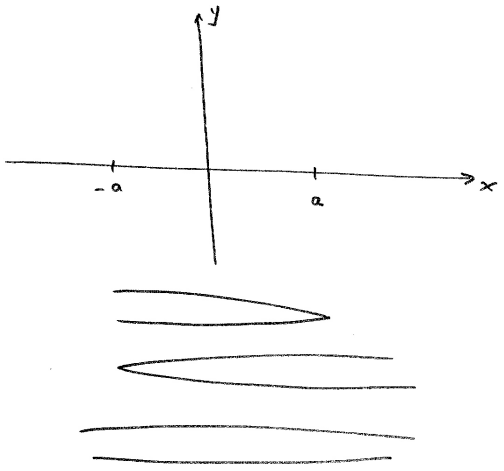

Fig. 3.5

As will be seen in the solution process, Equation (3.23) does not have a unique solution. The physical meaning of the nonuniqueness, as shown in Figure 3.5, is that an infinite number of traction free cracks with nonzero opening at the endpoints $x=\pm a$ satisfy Equation (3.23). Closure of both crack tips leads to a unique solution of Equation (3.23)

through the *single valued displacement* conditions $g(-a) = g(a) = 0$. These can be written in terms of the dislocation density through Equation (3.22b)

$$g(-a) = \int_{-a}^{a} B(\xi) d\xi = 0$$

(3.24a)

$$g(a) = \int_{a}^{a} B(\xi) d\xi = 0$$

(3.24b)

Equation (3.24a) is trivial, so only Equation (3.24b) is needed as a supplement to Equation (3.23).

Equations (3.23) and (3.24a) are nondimensionalized through the substitutions $t \equiv \frac{\xi}{a}$, $s \equiv \frac{x}{a}$ and $\hat{B}(t) \equiv \frac{2\mu}{\pi(\kappa+1)\sigma^{\infty}} B(t)$

$$\int_{-1}^{1} \frac{\hat{B}(t) dt}{t - s} = 1 \qquad |s| < 1$$

(3.25a)

$$\int_{-1}^{1} \hat{B}(t) dt = 0$$

(3.25b)

Symmetry about the $y-$axis eliminates solutions bounded at one end and singular at the other. The bounded at both end solutions does not satisfy the consistency condition (3.9), since

$$\int_{-1}^{1} \frac{dt}{\sqrt{1 - t^2}} \neq 0$$

(3.26)

which follows from the fact that the integrand is an even function.

The solution is therefore

$$\hat{B}(t) = -\frac{1}{\pi^2\sqrt{1-s^2}}\int_{-1}^{1}\frac{\sqrt{1-t^2}}{t-s}\,dt + \frac{C}{\sqrt{1-s^2}} = -\frac{1}{\pi^2\sqrt{1-s^2}}\int_{-1}^{1}\frac{\left(1-t^2\right)}{\sqrt{1-t^2}\left(t-s\right)}\,dt + \frac{C}{\sqrt{1-s^2}} \tag{3.27}$$

From Table 3.2 it follows that

$$\hat{B}(s) = \frac{s}{\pi\sqrt{1-s^2}} + \frac{C}{\sqrt{1-s^2}} \tag{3.28}$$

Substituting Equation (3.28) into (3.25b)

$$\int_{-1}^{1}\frac{\xi}{\pi\sqrt{1-\xi^2}}\,d\xi + C\int_{-1}^{1}\frac{d\xi}{\sqrt{1-\xi^2}} = 0 \tag{3.29}$$

The first integral on the left hand side of Equation (3.29) is equal to zero, since the integrand is an odd function. The second integral, on the other hand, is not equal to zero, since the integrand is an even function. Therefore the equation is satisfied only by $C = 0$.

The dislocation density becomes

$$B(x) = \frac{(\kappa+1)\sigma^{\infty}}{2\mu}\frac{x}{\sqrt{a^2-x^2}} \tag{3.30}$$

The crack opening displacement is obtained as

$$g(x)=\int_x^a B(\xi)d\xi=\frac{(\kappa+1)\sigma^\infty}{2\mu}\int_x^a\frac{\xi}{\sqrt{a^2-\xi^2}}d\xi=\frac{(\kappa+1)\sigma^\infty}{2\mu}\sqrt{a^2-x^2}$$

(3.31)

The stress intensity factor can be calculated by first evaluating the stress ahead of the crack along $y=0$

$$\sigma_{yy}=\sigma^\infty+\frac{\sigma^\infty}{\pi}\int_{-a}^a\frac{\xi}{\sqrt{a^2-x^2}(x-\xi)}d\xi=\sigma^\infty\left[1+\frac{1}{\pi}\int_{-1}^1\frac{t}{\sqrt{1-t^2}(s-t)}dt\right]$$

(3.32)

Using Table 3.2

$$\sigma_{yy}=\sigma^\infty\frac{|x|}{\sqrt{x^2-a^2}}\qquad |x|>a$$

(3.33)

The stress intensity factor calculated as

$$K_I=\lim_{x\to a^+}\left[\sqrt{2\pi(x-a)}\sigma_{yy}\right]=\lim_{x\to a^+}\left[\sqrt{2\pi(x-a)}\sigma^\infty\frac{|x|}{\sqrt{(x-a)}\sqrt{(x+a)}}\right]=\sigma^\infty\sqrt{\pi a}$$

(3.34)

Numerical Solution of Singular Integral Equations

In most problems the resulting integral equations cannot be solved analytically. In this section a very simple and accurate method is presented that can be used to obtain numerical solutions of the general form of the singular integral equation of the first kind

$$\int_{-1}^{1} \frac{\varphi(t)dt}{t-x} + \int_{-1}^{1} \varphi(t)K(x,t)dt = f(x) \qquad -1 < x < 1 \qquad (3.35)$$

The kernel K that appears in Equation (3.35) is a well behaved function that takes care of additional boundary conditions that arise from finite geometry and/or interaction effects. Some examples will be described subsequently. Without loss of generality, consider the solution singular at both endpoints, for which the unknown function can be written as

$$\varphi(t) = \frac{\varphi_{reg}(t)}{\sqrt{1-t^2}} \tag{3.36}$$

where φ_{reg} is a bounded function. Equation (3.35) can then be written as

$$\int_{-1}^{1} \frac{\varphi_{reg}(t)dt}{\sqrt{1-t^2}(t-x)} + \int_{-1}^{1} \frac{\varphi_{reg}(t)K(x,t)}{\sqrt{1-t^2}} dt = f(x) \qquad -1 < x < 1 \tag{3.37}$$

A very accurate and simple method for solving Equation (3.37) numerically was developed by Erdogan and Gupta. This method relies on properties of Chebychev polynomials of the first and second kind, which are defined, respectively, as

$$T_j(t) \equiv \cos(j\theta) \tag{3.38a}$$

$$U_j(x) \equiv \frac{\sin([j+1]\phi)}{\sin\phi} \tag{3.38b}$$

where

$$t \equiv \cos\theta \qquad 0 \le \theta \le \pi \tag{3.39a}$$

$$x \equiv \cos\phi \qquad 0 \le \phi \le \pi \tag{3.39b}$$

The roots of these polynomials, obtained by setting Equations (3.38) equal to zero, are given by

$$\theta_k = \frac{(2k-1)\pi}{2n} \qquad k = 1,2,\ldots n \tag{3.40a}$$

$$\phi_r = \frac{r\pi}{n} \qquad r = 1,2,\ldots(n-1) \tag{3.40b}$$

and are shown schematically in Figure 3.6.

The method relies on the representation

$$\int_{-1}^{1} \frac{T_j(t)dt}{\sqrt{1-t^2}(t-x_r)} = \frac{\pi}{n}\sum_{k=1}^{n} \frac{T_j(t_k)}{t_k - x_r} \tag{3.41}$$

which follows from the identities that relate the Chebychev polynomial of the first kind of order j to the Chebychev polynomial of the second kind of order $j-1$

$$\int_{-1}^{1} \frac{T_j(t)dt}{\sqrt{1-t^2}(t-x)} = \pi U_{j-1}(x) \tag{3.42a}$$

$$U_{j-1}(\cos\phi_r) = \frac{1}{n}\sum_{k=1}^{n} \frac{T_j(\cos\theta_k)}{\cos\theta_k - \cos\phi_r} \tag{3.42b}$$

The numerical procedure starts with the approximation of the regular part of the unknown function in terms of the Chebychev polynomials of the first kind

$$\varphi_{reg}(t) = \varphi_{reg}(\cos\theta) \approx \sum_{j=0}^{n} B_j T_j(t) \tag{3.43}$$

where the B_j are constant coefficients. Multiplying Equation (3.41) by B_j and summing on j leads to the following representation for the first integral in Equation (3.37)

$$\int_{-1}^{1} \frac{\varphi_{reg}(t)dt}{\sqrt{1-t^2}(t-x_r)} = \frac{\pi}{n}\sum_{k=1}^{n} \frac{\varphi_{reg}(\cos\theta_k)}{\cos\theta_k - \cos\phi_r} \qquad r = 1,2,\ldots,(n-1) \tag{3.44}$$

The next approximation involves the second integral in Equation (3.37)

$$\int_{-1}^{1} \varphi_{reg}(t) K(x_r, t) \frac{dt}{\sqrt{1-t^2}} = \int_0^{\pi} \varphi_{reg}(t) K(x_r, t) d\theta \approx \frac{\pi}{n} \sum_{k=1}^{n} \varphi_{reg}(\cos\theta_k) K(\cos\phi_r, \cos\theta_k)$$

(3.45)

Equations (3.44) and (3.45) transform the singular integral equation into a system of algebraic equations for the unknown values of the regular part of the unknown function

$$\frac{\pi}{n} \sum_{k=1}^{n} \varphi_{reg}(t_k) \left[\frac{1}{t_k - x_r} + K(t_k, x_r) \right] = f(x_r) \qquad r = 1,2,...,(n-1)$$

(3.46)

where $t_k = \cos\theta_k$ and $x_r = \cos\phi_r$.

Because there are n unknown nodal values of φ_{reg} and only $(n-1)$ equations, an additional condition that renders the solution unique must be supplemented to the system. As explained in the previous examples, the uniqueness condition is of the form

$$\int_{-1}^{1} \varphi(t) dt = A$$

(3.47)

which is approximated as

$$\int_{-1}^{1} \frac{\varphi_{reg}(t) dt}{\sqrt{1-t^2}} \approx \frac{\pi}{n} \sum_{k=1}^{n} \varphi_{reg}(t_k) = A \qquad (3.48)$$

For a given problem, the solution of Equations (3.46) and (3.48) provides n values of φ_{reg} at points $t_1 ... t_n$ within the interval $-1 < t < 1$. The values of φ_{reg} at the endpoints $t = \pm 1$, which for crack problems is proportional to the stress intensity factor, can be evaluated in terms of the calculated nodal values by using Legendre polynomial

interpolation to find a unique polynomial that takes on the same values as φ_{reg} at points $t_1 ... t_n$. This procedure, which is described in detail by Rivlin, provides the formulas

$$\varphi_{reg}(1) = \frac{1}{n}\sum_{k=1}^{n}(-1)^{k-1}\varphi_{reg}(t_k)\sqrt{\frac{1-t_k}{1+t_k}} = \frac{1}{n}\sum_{k=1}^{n}(-1)^{k}\varphi_{reg}(t_k)\cot\left(\frac{[2k-1]\pi}{4n}\right) \qquad (3.49a)$$

$$\varphi_{reg}(-1) = \frac{1}{n}\sum_{k=1}^{n}(-1)^{k+n}\varphi_{reg}(t_k)\sqrt{\frac{1+t_k}{1-t_k}} = \frac{1}{n}\sum_{k=1}^{n}(-1)^{k+n}\varphi_{reg}(t_k)\tan\left(\frac{[2k-1]\pi}{4n}\right) \qquad (3.49b)$$

Example: A Crack Perpendicular to a Bimaterial Interface

Figure 3.7a shows a Mode-I crack of length $2a$ perpendicular to the perfectly bonded interface between two isotropic half-planes. The crack is in material 1. Henceforth superscript and subscript 1 (2) represents "of material 1 (2)". The loading consists of uniform pressure σ along the crack surfaces. The distance from the left tip of the crack to the interface is δ. Because of its relevance to fracture of composite materials, the problem of calculating the stress intensity factors for this configuration has been addressed by several authors, including Erdogan *et al.*, Atkinson, and Romeo and Ballarini.

This elasticity problem can be formulated using the Green's function for the edge dislocation with Burgers vector parallel to the interface, as shown in Figure 3.7b. The Airy stress functions for mediums 1 and 2 are given by Dundurs

$$\chi^{(1)} = -\frac{2\mu_1}{\pi(\kappa_1+1)}b_x\left[r_1\log r_1\cos\theta_1 + \frac{\alpha+\beta^2}{1-\beta^2}r_2\log r_2\cos\theta_2 - \frac{1+\alpha}{1-\beta^2}\beta r_2\theta_2\sin\theta_2 - \frac{2(\alpha-\beta)}{1-\beta^2}\xi\left(\log r_2 - \frac{\cos\theta_2}{2} + \frac{\xi}{r}\cos\theta_2\right)\right] \qquad (3.50a)$$

$$\chi^{(2)} = -\frac{2\mu_2}{\pi(\kappa_2+1)}\frac{1+\alpha}{1-\beta^2}b_x\left[r_1\log r_1\cos\theta_1 + \beta\left(r_1\theta_1\sin\theta_1 + 2\xi\log r_1\right)\right] \qquad (3.50b)$$

where the Dundurs constants are defined by

$$\alpha \equiv \frac{\mu_2(\kappa_1+1)-\mu_1(\kappa_2+1)}{\mu_2(\kappa_1+1)+\mu_1(\kappa_2+1)} \tag{3.51a}$$

$$\beta \equiv \frac{\mu_2(\kappa_1-1)-\mu_1(\kappa_2-1)}{\mu_2(\kappa_1+1)+\mu_1(\kappa_2+1)} \tag{3.51b}$$

If the dislocation is placed in material 2, the corresponding Airy stress functions are obtained by replacing α and β in Equations (3.50) with $-\alpha$ and $-\beta$. The stress and displacement fields associated with these stress functions satisfy the jump conditions at point $(0,\xi)$ and the continuous displacement and continuous traction conditions along the interface

$$\sigma_{yy}^2(x,0) = \sigma_{yy}^1(x,0) \tag{3.52a}$$

$$\sigma_{xy}^2(x,0) = \sigma_{xy}^1(x,0) \tag{3.52b}$$

$$u_x^2(x,0) = u_x^1(x,0) \tag{3.52c}$$

$$u_y^2(x,0) = u_y^1(x,0) \tag{3.52d}$$

The relevant stress along the crack line is given by

$$\sigma_{xx}^1(0,y) = -\frac{2\mu_1}{\pi(\kappa_1+1)} b_x \left[\frac{1}{y-\xi} + K(y,\xi) \right] \tag{3.53}$$

with

$$K(y,\xi) \equiv \left[\frac{\alpha+\beta^2}{1-\beta^2}\frac{1}{y+\xi} + \frac{2(\alpha-\beta)}{1+\beta}\frac{\xi(y-\xi)}{(y+\xi)^3} \right] \tag{3.54}$$

Replacing the discrete dislocation with a distribution and setting the total stress equal to the prescribed uniform pressure leads to

$$\frac{2\mu_1}{\pi(\kappa_1+1)}\int_{\delta}^{\delta+2a} B(\xi)\left[\frac{1}{y-\xi}+K(y,\xi)\right]d\xi=\sigma \qquad \delta\le y\le\delta+2a$$

(3.55)

and the single valued displacement condition

$$\int_{\delta}^{\delta+2a} B(\xi)d\xi=0 \tag{3.56}$$

Note that the kernel K appearing in the integral equation is well behaved as long as the left crack tip does not touch the interface $(\delta=0)$. If it does, then the term $\frac{1}{y+\xi}$ becomes singular and the singularity at the left crack tip is different than square root. The resulting integral equation is said to have a *generalized Cauchy kernel*, according to Erdogan.

Equations (3.55) and (3.56) can be cast in the form of Equation (3.35) and (3.47) by means of the transformations $t\equiv\frac{\xi-(a+\delta)}{a}$, $s\equiv\frac{y-(a+\delta)}{a}$, $\hat{B}(t)\equiv\frac{2\mu_1}{\pi(\kappa_1+1)\sigma}B(t)$.

The result is

$$\int_{-1}^{1}\hat{B}(t)\left[\frac{1}{s-t}+K(s,t)\right]dt=1 \qquad -1\le s\le 1 \tag{3.57a}$$

$$\int_{-1}^{1}\hat{B}(t)dt=0 \tag{3.57b}$$

with

$$K(s,t) \equiv \left[\frac{\alpha+\beta^2}{1-\beta^2} \frac{1}{t+s+2+2\dfrac{\delta}{a}} + \frac{2(\alpha-\beta)}{1+\beta} \frac{\left(t+1+\dfrac{\delta}{a}\right)(s-t)}{\left(t+s+2+2\dfrac{\delta}{a}\right)^3} \right] \tag{3.58}$$

The discretized matrix form of the singular integral equation (3.57a) is the $n-1 \times n$ matrix

$$\frac{\pi}{n} \begin{bmatrix} \dfrac{1}{t_1-s_1}+K(t_1,s_1) & \dfrac{1}{t_2-s_1}+K(t_2,s_1) & \ldots & \dfrac{1}{t_n-s_1}+K(t_n,s_1) \\ \dfrac{1}{t_1-s_2}+K(t_1,s_2) & \dfrac{1}{t_2-s_2}+K(t_2,s_2) & \ldots & \dfrac{1}{t_n-s_2}+K(t_n,s_2) \\ \ldots & \ldots & \ldots & \ldots \\ \dfrac{1}{t_1-s_{n-1}}+K(t_1,s_{n-1}) & \dfrac{1}{t_2-s_{n-1}}+K(t_2,s_{n-1}) & \ldots & \dfrac{1}{t_n-s_{n-1}}+K(t_n,s_{n-1}) \end{bmatrix} \begin{Bmatrix} \hat{B}_{reg}(t_1) \\ \hat{B}_{reg}(t_2) \\ \ldots \\ \hat{B}_{reg}(t_n) \end{Bmatrix} = \begin{bmatrix} 1 \\ 1 \\ \ldots \\ 1 \end{bmatrix} \tag{3.59}$$

which is made square with the supplemental discretized version of single valued displacement condition (3.57b)

$$\begin{bmatrix} 1 & 1 & \ldots & 1 \end{bmatrix} \begin{Bmatrix} \hat{B}_{reg}(t_1) \\ \hat{B}_{reg}(t_2) \\ \ldots \\ \hat{B}_{reg}(t_n) \end{Bmatrix} = 0 \tag{3.60}$$

The solution of system (3.59) and (3.60), together with the Legendre formulas (3.49), provide the value of the regular part of the dislocation density at the crack tips, which are related next to the stress intensity factors. Without loss of generality, consider the stress intensity factor of the crack tip closest to the interface.

The crack opening displacement very near the tip of a Mode-I crack is given by the asymptotic form derived in Chapter 2

$$g(r) = \frac{(\kappa_1 + 1)K_I}{2\mu_1}\sqrt{\frac{r}{2\pi}} \tag{3.61}$$

The dislocation density follows from Equation (3.61)

$$B(r) = -\frac{(\kappa_1 + 1)}{4\mu_1\sqrt{2\pi}}\frac{K_I}{\sqrt{r}} \tag{3.62}$$

Equating this last equation, as $r = \xi - a = a(1+t) \to 0$, with the numerical approximation

$$\hat{B}(t) \equiv \frac{2\mu_1}{\pi(\kappa_1 + 1)\sigma}B(t) = \frac{\hat{B}_{reg}(t)}{\sqrt{1-t^2}} \tag{3.63}$$

provides,

$$B(t) = -\frac{(\kappa_1 + 1)}{4\mu_1\sqrt{2\pi}}\frac{K_I}{\sqrt{1+t}\sqrt{a}} = \frac{\pi(\kappa_1 + 1)\sigma}{2\mu_1}\frac{\hat{B}_{reg}(-1)}{\sqrt{1+t}\sqrt{1-t}} \tag{3.64}$$

or

$$\frac{K_I}{\sigma\sqrt{\pi a}} = -2\pi\hat{B}_{reg}(-1) \tag{3.65}$$

A Crack Very Close to a Bimaterial Interface

A. Romeo
Graduate Student.

R. Ballarini
Associate Professor.

Department of Civil Engineering,
Case Western Reserve University,
Cleveland, OH 44106-7201

This paper presents the plane elastostatics analysis of a semi-infinite crack perpendicular to a perfectly bonded bimaterial interface. Both cases of the crack approaching the interface and penetrating the interface are addressed. The distance from the tip of the crack to the interface is δ. A singular integral equation approach is used to calculate the stress intensity factor, K_I, and the crack-opening displacement at the interface, η, as functions of δ, the Dundurs parameters α and β, and the stress intensity factor k_I associated with the same crack terminating at the interface (the case $\delta = 0$). The results are presented as $K_I = k_I \delta^{1/2-\lambda} f(\alpha, \beta)$ and $\eta = C k_I \delta^{1-\lambda} \tilde{\eta}(\alpha, \beta)$ where λ is the strength of the stress singularity associated with $\delta = 0$, f and $\tilde{\eta}$ are functions calculated numerically and C is a material constant. These results can be used to determine the stress intensity factor and crack opening displacement of cracks of finite length 2a with one tip at a distance δ from the interface for $\delta/a \ll 1$. The selected results presented for a crack loaded by a uniform far-field tension in each half-plane show that the stress intensity factors approach their limits at a relatively slow rate.

1 Introduction

Consider the plane elastostatics problem shown in Fig. 1(*a*). A Mode I crack of length $2a$ is perpendicular to the perfectly bonded interface between two isotropic half-planes with shear moduli μ_i and Poisson's ratios ν_i, $i = 1, 2$. The distance from the left tip of the crack to the interface is δ. Because of its relevance to fracture of composite materials, the problem of calculating the stress intensity factors for this configuration has been addressed by several authors (Erdogan et al., 1973; Atkinson, 1975). It is well known that this elasticity problem can be formulated using the Green's function for the stress produced along the crack line by an edge dislocation. This procedure leads to the following singular integral equation and uniqueness condition:

$$\frac{2\mu_1}{\pi(\kappa_1+1)}\int_{\delta}^{\delta+2a} b(\xi)\left[\frac{1}{y-\xi}+\frac{\alpha+\beta^2}{1-\beta^2}\frac{1}{y+\xi}+\frac{2(\alpha-\beta)}{1+\beta}\frac{\xi(y-\xi)}{(y+\xi)^3}\right]d\xi = -\sigma_{xx}(y)$$

$$\int_{\delta}^{\delta+2a} b(\xi)\,d\xi = 0 \quad \delta \le y, \xi \le \delta + 2a \tag{1}$$

where σ_{xx} is the stress along the crack line induced by the remote loading in the uncracked body, α and β are the Dundurs parameters (Dundurs, 1969)

$$\alpha = \frac{\mu_2(\kappa_1+1)-\mu_1(\kappa_2+1)}{\mu_2(\kappa_1+1)+\mu_1(\kappa_2+1)};$$

$$\beta = \frac{\mu_2(\kappa_1-1)-\mu_1(\kappa_2-1)}{\mu_2(\kappa_1+1)+\mu_1(\kappa_2+1)}$$

$\kappa_i = 3 - 4\nu_i$ for plane strain and $\kappa_i = (3-\nu_i)/(1+\nu_i)$ for plane stress. The unknown dislocation density $b(\xi)$ is defined in terms of the crack opening displacement $[u_x(\xi)]$ as

$$b(\xi) \equiv -\frac{\partial}{\partial \xi}[u_x]. \tag{2}$$

The first equation in (1) represents the zero traction condition along the crack surfaces, while the second enforces single-valued displacements (both crack tips are closed). In the following, the loading is taken as uniform remote tension in each half-plane, $\sigma^{(1)}$ and $\sigma^{(2)}$, such that

$$\sigma^{(2)} = \frac{1+\alpha}{1-\alpha}\sigma^{(1)} \tag{3}$$

and therefore $\sigma_{xx} = \sigma^{(1)}$ in Eq. (1).

The ratio $\delta/2a$ enters in the kernel of the singular integral Eq. (1) in such a way that stress intensity factor values calculated using a direct numerical solution inevitably lose accuracy for $\delta/2a \ll 1$. Indeed, the smallest ratio for which Erdogan et al. (1973) present results is $\delta/2a = 0.05$. Their results showed that as $\delta \to 0$ the stress intensity factor of the crack tip closest to the interface approaches zero when $\mu_2 > \mu_1$ and infinity when $\mu_1 > \mu_2$. These limits result from the discontinuous change in the order of the stress singularity as δ becomes equal to zero. As will be explained in the next section, for $\delta = 0$ and $\mu_2 > \mu_1$ the stress ahead of the crack tip is of the order $k_I r^{-\lambda}$ with $\lambda < \frac{1}{2}$. This weaker singularity in effect reduces to zero, as $\delta \to 0$, the amplitude K_I of the square root singularity associated with $\delta \neq 0$. For $\mu_1 > \mu_2$, $\lambda > \frac{1}{2}$, and similar arguments explain why K_I increases to infinity as $\delta \to 0$. Assuming linear elastic fracture mechanics these limits imply that the crack reaches the interface at infinite load for $\mu_2 > \mu_1$ and zero load for $\mu_1 > \mu_2$.

As a first step toward the development of physically sound propagation criteria for interface cracks, this paper is concerned with determining, as functions of the elastic mismatch, the rate at which the square root singularity approaches the limits discussed above. To this end the problem is formulated asymptotically in terms of a semi-infinite crack in which the only length parameter is δ.

The approach used is essentially the same as that used by Hutchinson et al. (1987) to study a crack very close to and parallel to a bimaterial interface. It relies on some relevant well-

Contributed by the Applied Mechanics Division of THE AMERICAN SOCIETY OF MECHANICAL ENGINEERS for publication in the ASME JOURNAL OF APPLIED MECHANICS.

Discussion on this paper should be addressed to the Technical Editor, Prof. Lewis T. Wheeler, Department of Mechanical Engineering, University of Houston, Houston, TX 77204-4792, and will be accepted until four months after final publication of the paper itself in the ASME JOURNAL OF APPLIED MECHANICS.

Manuscript received by the ASME Applied Mechanics Division, July 2, 1993; final revision, May 3, 1994. Associate Technical Editor: D. M. Parks.

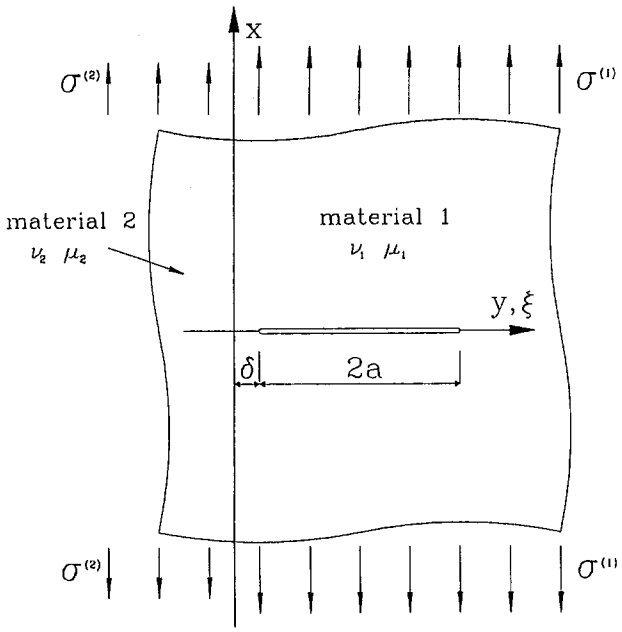

Fig. 1(*a*)

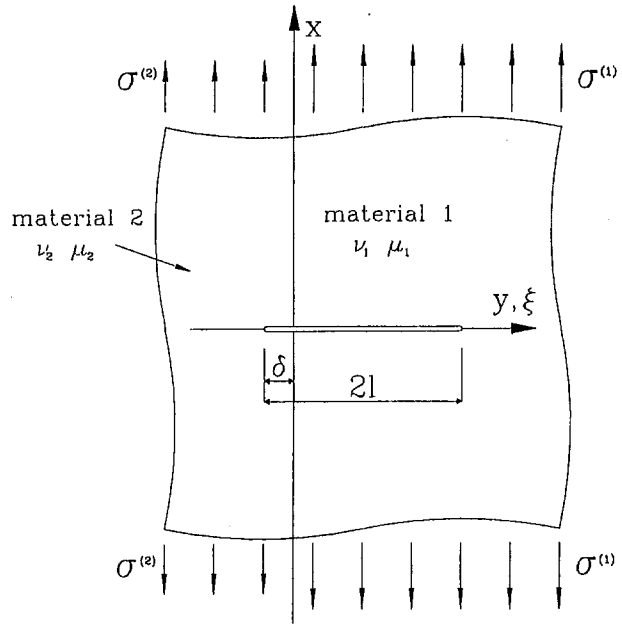

Fig. 1(*b*)

Fig. 1 Finite length crack (*a*) approaching and (*b*) penetrating a bimaterial interface

known results for the asymptotic behavior of the stresses and crack-opening displacements in the vicinity of the tip of a crack impinging on a bimaterial interface. These are reviewed briefly in the next section. The solution of the semi-infinite crack problem is discussed in the third section and an example of how the asymptotic analysis can be applied to the problem of Fig. 1(*a*) is provided in the 4th section. The last section extends the method to the case of a finite crack that penetrates a distance δ through the interface, Fig. 1(*b*).

2 Finite Crack Terminating at the Interface

The results of the Williams technique analysis for a crack terminating at the interface ($\delta = 0$ in Fig. 1(*a*)) show that the traction ahead of the crack tip is characterized by

$$\lim_{y\to 0^-} \{\sigma_{xx}^{(2)}(y)\} = \frac{k_I}{\sqrt{2\pi}}(-y)^{-\lambda} \tag{4}$$

where superscript (i) denotes "in material (i)," k_I is the stress intensity factor, and $\lambda (0 \le \lambda < 1)$ is the root of the equation derived by Zak and Williams (1963)

$$\cos(\lambda\pi) = \frac{2(\beta - \alpha)}{(1 + \beta)}(1 - \lambda)^2 + \frac{\alpha + \beta^2}{1 - \beta^2}. \tag{5}$$

The loci of constant λ in the α-β plane are shown in Fig. 2(*a*). As pointed out by Dundurs (1970), this figure clearly illustrates that for $\alpha \to 1$ the quantity λ is more sensitive to the mismatch in the Poisson's ratios, while for $\alpha \to -1$ it is more sensitive to the mismatch in the shear moduli.

Another important result from the Williams analysis relates the crack-opening displacement (COD), $[u_x^{(1)}(y)]$, to the stress ahead of the crack, i.e.,

$$\lim_{y\to 0^+} \{\sigma_{xx}^{(2)}(-y)\} = \lim_{y\to 0^+} \left\{-\psi \frac{\partial}{\partial y}[u_x^{(1)}(y)]\right\}$$

$$= \lim_{y\to 0^+} \{\psi b(y)\} \tag{6}$$

where the bimaterial parameter ψ is defined as

$$\psi \equiv \frac{2\mu_1}{(\kappa_1 + 1)} \frac{1}{\sin(\lambda\pi)} \left(\frac{1 + \alpha}{1 - \beta^2}\right)[1 - 2\beta(\lambda - 1)]. \tag{7}$$

Equation (6) allows the determination of the stress intensity factor of a crack of length $2a$ in terms of the dislocation density as

$$k_I = \lim_{y\to 0^+} \{\psi\sqrt{\pi} a^{\lambda} \tilde{b}(y)\} \tag{8}$$

in which

$$\tilde{b}(y) = a^{-(\lambda+1/2)} b(y) y^{\lambda} (2a - y)^{1/2}$$

is the regular part of the dislocation density $b(y)$.

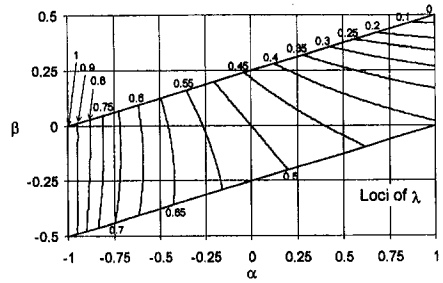

Fig. 2(*a*)

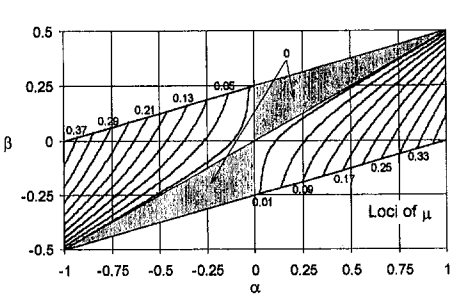

Fig. 2(*b*)

Fig. 2 Loci of (*a*) constant λ and (*b*) constant μ in the α-β plane

It is worth noting that (8) could also be derived by studying the behavior near the crack tip of the generalized Cauchy-type integral that represents the stress $\sigma_{xx}^{(2)}$.

3 Semi-infinite Crack Analysis

Consider a semi-infinite crack perpendicular to the interface and terminating at a distance δ from it. The COD at a point $r = y - \delta$ very close to the crack tip ($r/\delta \ll 1$) is given by $[u_x] \propto K_I r^{1/2}$, where K_I is the stress intensity factor. For $r/\delta \gg 1$ the COD approaches the one associated with the crack tip impinging on the interface ($\delta = 0$), i.e., $[u_x] \propto k_I r^{1-\lambda}$. The physical meaning is that since δ is very small the COD in the far-field is indistinguishable from the COD of the same crack impinging on the interface.

Linearity and dimensional considerations (δ is the only characteristic length) demand that

$$\frac{K_I}{k_I \delta^{1/2-\lambda}} = f(\alpha, \beta) \tag{9}$$

where f is a function of the Dundurs parameters only. This type of argument was employed by Hutchinson et al. (1987) and He and Hutchinson (1989).

It should be noted that this last result was derived by Atkinson (1975) by applying the Mellin transform to the integral equation

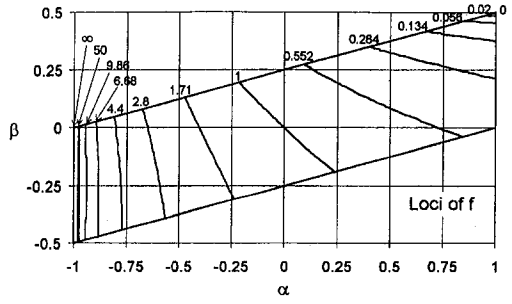

Fig. 3(*a*)

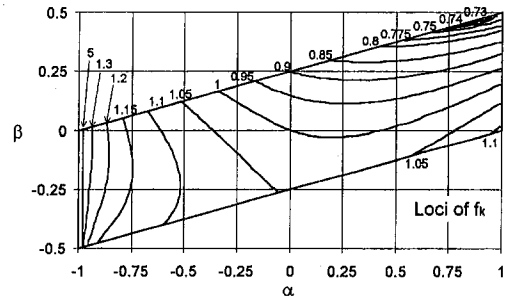

Fig. 3(*b*)

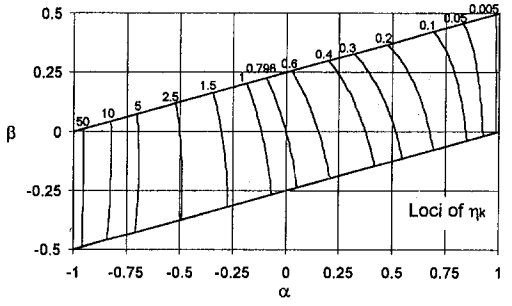

Fig. 3(*c*)

Fig. 3 Loci of (*a*) constant f, (*b*) constant f^*, and (*c*) constant $\hat{\eta}$ in the α-β plane

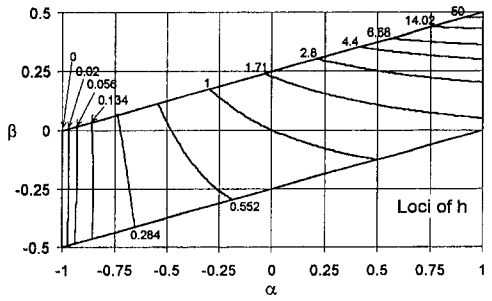

Fig. 4 Loci of constant h in the α, β-plane

and using the Wiener-Hopf technique. He showed that the stresses ahead of the crack are given by (using the notation in his paper)

$$\sigma_{xx} \approx \epsilon^{1/2} r^{-1/2} \{ \sum_{k=1}^{N} A_k \epsilon^{s_k' - 2} + O(\epsilon^{3s_1' - 4}) \} \tag{10}$$

where the A_k are constants independent of ϵ, α_1 and β are material constants (not to be confused with the Dundurs parameters), and s_k' are the N real roots ($\mathrm{Re}(s) > 1$) of the equation

$$\cos(\pi s) + \alpha_1 - \beta(s-1)^2 = 0. \tag{11}$$

It can be easily shown that the dominant term of the stress given by (10) corresponds to that produced by the stress intensity factor defined by relation (9), the constants A_k being identified with the values of $k_I f(\alpha, \beta)$, and $s_1' = 2 - \lambda$. Atkinson developed his solution for a constant pressure loading, but did not present numerical results for coefficients A_k. The main contribution of the present paper is that it presents complete results for these universal functions.

As will be described in the next section, (9) provides a powerful tool for the asymptotic analysis of finite length cracks approaching a bimaterial interface. The values of the function $f(\alpha, \beta)$ were calculated by integrating numerically (1) for $2a = \infty$. The details of the solution procedure are given in the Appendix.

The loci of constant f in the α-β plane are shown in Fig. 3(*a*). It is interesting to note that the sensitivity of f to changes in shear moduli and Poisson ratios is qualitatively the same as that of the singularity coefficient λ.

4 Finite Crack Very Close to the Interface

The numerical scheme used for solving the singular integral equation for the finite crack depicted in Fig. 1(*a*) becomes unstable when the ratio $\delta/2a$ assumes very small values. For these cases, an indirect method based on asymptotical analysis is recommended for computing the stress intensity factor. This approach relies on the combination of (9) and the stress intensity factor k_I associated with the finite crack terminating at the interface ($\delta = 0$).

As an example, consider the case of a crack acted upon by a uniform remote tension field in the two connected half-planes according to (3). As shown in the Appendix the stress intensity factor k_I can be represented as

$$\frac{k_I}{\sigma\sqrt{\pi a^{\lambda}}} = h(\alpha, \beta). \tag{12}$$

The loci of constant h in the α-β plane are shown in Fig. 4. It is observed that the stress intensity factor for this problem is yet another parameter that is more sensitive to the mismatch in the Poisson's ratios for $\alpha \to 1$, while for $\alpha \to -1$ it is more sensitive to the mismatch in the shear moduli. Combining (9) and (12) leads to the following expression for the stress intensity factor of a crack of length $2a$ at a distance δ from the interface:

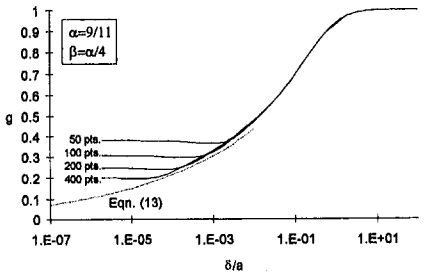

Fig. 5(*a*)

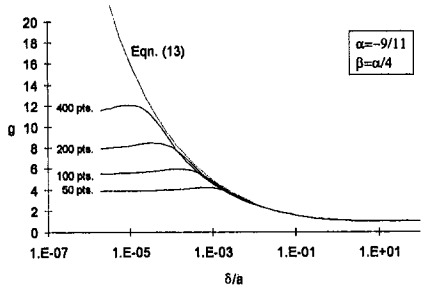

Fig. 5(*b*)

Fig. 5 Numerical instability and transition to the asymptotical solution of g for small δ/a ratios for (*a*) $\alpha = 4\beta = \frac{9}{11}$ and (*b*) $\alpha = 4\beta = -\frac{9}{11}$

$$\frac{K_I}{\sigma\sqrt{\pi}a^{1/2}} = g(\alpha, \beta) = \left(\frac{\delta}{a}\right)^{1/2-\lambda} f(\alpha, \beta)h(\alpha, \beta); \quad \delta/a \to 0. \tag{13}$$

Selected results for the asymptotic value of the stress intensity factor as calculated using (13) are presented in Figs. 5(*a*) and 5(*b*) for $\alpha = 4\beta = \pm\frac{9}{11}$; these values of the Dundurs parameters include $\nu_1 = \nu_2$ and $\mu_2/\mu_1 = 10$ or $\mu_1/\mu_2 = 10$. The solid lines in these plots are the values of the stress intensity factor calculated through a direct numerical solution of (1) along the finite interval. The procedure used for these calculations is outlined in the Appendix. As expected the direct solution for a given number of integration points breaks down as the distance from the crack tip to the interface assumes relatively small values. The asymptotic solution approaches the envelope defined by the value of δ/a at which the direct numerical solution, for a given value of integration points, becomes unstable.

The most interesting results of this analysis is that the stress intensity factor approaches the aforementioned limits at relatively slow rates. For significant elastic mismatch, $\alpha = 4\beta = \frac{9}{11}$, the stress intensity factor for $\delta/a = 0.001$ is approximately 30 percent of the nominal value associated with no interface. These results suggest that although the stress intensity factor for $\mu_2 > \mu_1$ approaches zero, this limit is associated with distances δ much smaller than the plastic zone that inevitably surrounds the crack tip. The leading edge of the plastic zone will thus reach the interface at a finite load. Perhaps more importantly, cracks in typical engineering materials will have extremely small δ values that will invalidate a continuum mechanics formulation.

5 Finite Crack Extending Through the Interface

The asymptotical technique described in the previous sections can be easily extended to other interface crack problems. The natural extension of the previous formulation is to a finite crack of length $2l = 2(a + b)$ that has extended beyond the interface a distance $\delta = 2b \ll l$ (Fig. 1(*b*)). This problem can be reduced to a set of coupled singular integral equations using the same Green's function approach that is used to derive (1) (Erdogan and Biricikoglu, 1973). These equations are written symbolically in terms of the dislocation densities $b^{(i)}(\xi)$ $(i = 1, 2)$:

$$A_1 \int_0^{2a} b^{(1)}(\xi)K_{1i}\,d\xi + A_2 \int_{-2b}^{0} b^{(2)}(\xi)K_{2i}\,d\xi = -\sigma^{(i)} \quad (i = 1, 2)$$

$$\int_0^{2a} b^{(1)}(\xi)d\xi + \int_{-2b}^{0} b^{(2)}(\xi)d\xi = 0 \tag{14}$$

where K_{ij} $(i, j = 1, 2)$ are Cauchy-type kernels. The first two Eqs. (14) represent the traction boundary conditions, while the third enforces single-valued displacements. The condition on the dislocation density required to insure compatibility at the interface is given by

$$\lim_{y\to 0^+} b^{(2)}(y)/b^{(1)}(-y) = F(\alpha, \beta, \mu) \tag{15}$$

where

$$F(\alpha, \beta, \mu) = \frac{(1+\alpha)\beta + (\alpha-\beta)\times(1-\beta)(-1+4\mu-2\mu^2) - (1-\beta^2)\cos(\mu\pi)}{(1+\alpha)(-1+2\beta-2\beta\mu)} \tag{16}$$

and μ is the power of the stress singularity, which satisfies the characteristic equation

$$(1-\beta^2)(1+\cos^2\mu\pi) + 2[2\alpha\beta - 1 - (2\alpha\beta - \beta^2)\cos\mu\pi] + 4\mu(2-\mu)[(\alpha-\beta)^2(1-\mu)^2 - \alpha\beta + \beta(\alpha-\beta)\cos\mu\pi] = 0.$$

The loci of constant μ are plotted in Fig. 2(*b*).

Again a direct solution of Eqs. (14) is inadequate for very small b/a ratios and an alternative approach is furnished by the asymptotical analysis. The reference problem is still the finite crack of length $2l$ terminating at the interface. The semi-infinite analysis on the other hand has to be redefined, since the crack tip is now located beyond the interface at a distance δ from it. As before, the far-field COD has to approach the one associated with no penetration, $[u_x] \propto k_I r^{1-\lambda}$, and in the vicinity of the crack tip the COD is given by $[u_x] \propto K_I r^{1/2}$. However, an additional requirement is that the COD at the interface be of the order $r^{1-\mu}$. Equation (9) still applies with $f(\alpha, \beta)$ replaced by the new function $f^*(\alpha, \beta)$ whose values are computed by solving numerically the proper set of integral equations (see Appendix); the loci of this function in the α-β plane are plotted in Fig. 3(*b*).

Combining (9) and (12) leads to the asymptotical expression of the stress intensity factor of a finite crack of length $2l$ the has penetrated in material 2 by the distance $\delta = 2b \ll l$

$$\frac{K_I}{\sigma^{(1)}\sqrt{\pi}l^{1/2}} = g^*(\alpha, \beta) = \left(\frac{2c}{1+c}\right)^{1/2-\lambda} f^*(\alpha, \beta)h(\alpha, \beta) \tag{17}$$

where

$$c = b/a.$$

The predictions of Eq. (17) are valid in the limit $\delta/l \to 0$. Figures 6 and 7 show the convergence of the nondimensional stress intensity factor values found by direct numerical integration to the asymptotic solution given by (17) for the two material combinations already used in the previous sections, $\alpha = \pm\frac{9}{11} = 4\beta$. Note that the for the case $\alpha = +\frac{9}{11} = 4\beta$, which corresponds to $\lambda = 0.347$, the rate of convergence is much slower than for $\alpha = -\frac{9}{11} = 4\beta$ $(\lambda = 0.755)$.

Note that the asymptotic analysis can be used to compute not only stress intensity factors but also other quantities such as the

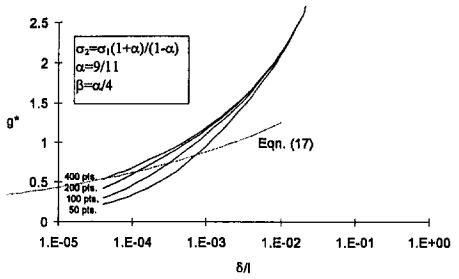

Fig. 6 Numerical instability and transition to the asymptotical solution of g^* for small δ/a ratios for $\alpha = 4\beta = \frac{9}{11}$

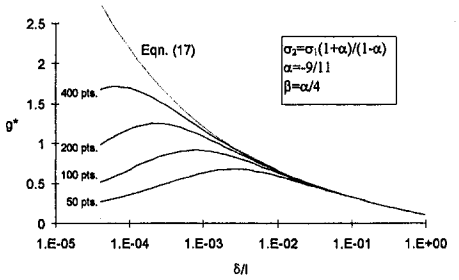

Fig. 7 Numerical instability and transition to the asymptotical solution of g^* for small δ/a ratios for $\alpha = 4\beta = -\frac{9}{11}$

crack-opening displacement at the interface. In fact, for a semi-infinite crack the COD at the interface, η, is given by

$$\eta = \frac{1 + \kappa_1}{2\mu_1} k_I \delta^{1-\lambda} \tilde{\eta}(\alpha, \beta) \tag{18}$$

where $\tilde{\eta}$ is a function of the Dundurs parameters whose loci are shown in Fig. 3(b). The asymptotic expression of the crack-opening displacement at the interface for the finite crack in Fig. 1(b) is then given by

$$\eta_f = -\sqrt{\pi}\phi_1 \delta \left(\frac{l}{\delta}\right)^{\lambda} h(\alpha, \beta)\tilde{\eta}(\alpha, \beta) \quad \delta/l \to 0 \tag{19}$$

where

$$\phi_1 = -\frac{\sigma^{(1)}(\kappa_1 + 1)}{2\mu_1}.$$

6 Conclusions

The numerical schemes that are used to solve integral equations describing the elastostatics problems of finite length cracks close to a bimaterial interface are not accurate when the relative distance δ from the crack tip to the interface becomes very small. An asymptotic analysis has been developed that provides accurate stress intensity factors for such problems and gives insight into their rate of change as $\delta \to 0$. For the case of a crack approaching or penetrating a bimaterial interface, it has been shown that the stress intensity factor at the leading crack tip approaches its limiting value at a slow rate. These results suggest that propagation criteria for such problems are associated with nonlinear processes. The technique presented in this paper can be used to solve a class of problems in which a small parameter leads to an unstable direct numerical solution of the governing equations.

Acknowledgment

This work was supported by the Lewis Research Center under Grant NAG3-856.

References

Atkinson, C., 1975, "On the Stress Intensity Factors Associated with Cracks Interacting with an Interface Between Two Elastic Media," *International Journal of Engineering Science,* Vol. 13, pp. 489–504.

Dundurs, J., 1969, "Elastic Interaction of Dislocations with Inhomogeneities," *Mathematical Theory of Dislocations,* T. Mura, ed., ASME, New York, pp. 70–114.

Dundurs, J., and Lee, S., 1970, "Stress Concentrations Due to Edge Dislocation Pile-ups in Two-phase Materials," *Scripta Metallurgica,* Vol. 4, pp. 313–314.

Erdogan, F., and Biricikoglu, V., 1973, "Two Bonded Half Planes with a Crack Going Through the Interface," *International Journal of Engineering Science,* Vol. 11, pp. 745–766.

Erdogan, F., Gupta, G. D., and Cook, T. S., 1973, "Numerical Solution of Singular Integral Equations," *Mechanics of Fracture,* Vol. 1, G. C. Sih, ed., Noordhoff International Publishing, pp. 368–425.

He, M. Y., and Hutchinson, J. W., 1989, "Crack Deflection at an Interface Between Dissimilar Elastic Materials," *International Journal Solids Structures,* Vol. 25, No. 9, pp. 1053–1067.

Hutchinson, J. W., Mear, M. E., and Rice, J. R., 1987, "Crack Paralleling an Interface Between Dissimilar Materials," ASME JOURNAL OF APPLIED MECHANICS, Vol. 54, No. 4, pp. 828–832.

Miller, G. R., and Keer, L. M., 1985, "A Numerical Technique for the Solution of Singular Integral Equations of the Second Kind," *Quarterly of Applied Mathematics,* Vol. 42, pp. 455–465.

Rubinstein, A. A., 1992, "Stability of the Numerical Procedure for Solution of Singular Integral Equations on Semi-Infinite Interval. Application to Fracture Mechanics," *Computers & Structures,* Vol. 44, No. 1/2, pp. 71–74.

Zak, A. R., and Williams, M. L., 1963, "Crack Point Stress Singularities at a Bi-Material Interface," ASME JOURNAL OF APPLIED MECHANICS, Vol. 30, pp. 142–143.

APPENDIX

Let

$$A_i = \frac{2\mu_i}{\pi(1 + \kappa_i)} \quad (i = 1, 2)$$

$$M = \frac{\alpha + \beta^2}{1 - \beta^2}; \quad N = \frac{2(\alpha - \beta)}{1 + \beta}; \quad S = \frac{1 + \alpha}{1 - \beta^2};$$

$$P = \frac{\alpha - \beta^2}{1 - \beta^2}; \quad Q = \frac{2(\alpha - \beta)}{1 - \beta}; \quad T = \frac{1 - \alpha}{1 - \beta^2};$$

$$K_{11}(\xi, y) = \frac{1}{y - \xi} + \frac{M}{y + \xi} + \frac{\xi(y - \xi)N}{(y + \xi)^3};$$

$$K_{12}(\xi, y) = S\left[\frac{1}{y - \xi} - 2\beta \frac{\xi}{(y - \xi)^2}\right];$$

$$K_{21}(\xi, y) = T\left[\frac{1}{y - \xi} + 2\beta \frac{\xi}{(y - \xi)^2}\right];$$

$$K_{22}(\xi, y) = \frac{1}{y - \xi} - \frac{P}{y + \xi} - \frac{\xi(y - \xi)Q}{(y + \xi)^3}. \tag{A1}$$

The following procedures were used to solve the integral equations numerically.

Crack of Length $2a$ at Distance δ From the Interface ($\delta \geq 0$)

The integral equations for this case are

$$A_1 \int_{\delta}^{\delta+2a} b(\xi) K_{11}(\xi, y) d\xi = -\sigma^{(1)}$$

$$\int_{\delta}^{\delta+2a} b(\xi) d\xi = 0 \quad \delta \leq y, \xi \leq \delta + 2a$$

The case $\delta = 0$ corresponds to a crack impinging on the interface. For the numerical computation these equations are rendered in nondimensional form and normalized in the interval $[-1, 1]$ by means of the transformations

$$t = \frac{\xi - (a+\delta)}{a}; \quad \zeta = \frac{y - (a+\delta)}{a};$$

$$\phi = -\frac{\sigma^{(1)}(\kappa_1 + 1)}{2\mu_1}.$$

The nondimensional stress intensity factor at the crack tip closest to the interface is given by

$$h(\alpha, \beta) = \frac{k_I}{\sigma^{(1)}\sqrt{\pi a^{\lambda}}} = \frac{\kappa_1 + 1}{2\mu_1}\psi\tilde{b}(-1); \quad \delta = 0 \quad \text{(A3)}$$

$$g(\alpha, \beta) = \frac{K_I}{\sigma^{(1)}\sqrt{\pi a^{1/2}}} = \tilde{b}(-1); \quad \delta > 0 \quad \text{(A4)}$$

where

$$\psi \equiv \frac{2\mu_1}{\kappa_1 + 1}\frac{1}{\sin(\lambda\pi)}\frac{1+\alpha}{1-\beta^2}[1 - 2\beta(\lambda - 1)]$$

and

$$\tilde{b}(t) = b(t)(1+t)^{\lambda}(1-t)^{1/2}$$

is the regular part of the dislocation density ($\lambda = \frac{1}{2}$ when $\delta > 0$). For the numerical solution of (A1), two methods were compared. $\tilde{b}(t)$ in the first method is represented as a truncated series of Jacobi polynomials (Erdogan et al., 1973), while in the second method it is expressed in terms of piecewise quadratic polynomials (Miller and Keer, 1985). The results shown a faster convergence for the latter method for which 64 integration points were necessary to capture three significant figures, versus 400 integration points necessary for the first method.

Semi-infinite Crack Whose Tip is at Distance δ From the Interface

The singular integral equation is the same as the first (A2) except that the upper limit $2a$ is replaced with ∞. The unknown dislocation density is represented in real coordinates as

$$b(\xi) = \frac{k_I}{\sqrt{2\pi}}\frac{\xi^{1/2}}{(\xi-\delta)^{1/2}\xi^{\lambda}}\left[\frac{\kappa_1+1}{2\mu_1}\tilde{b}(\xi) + w(\xi)\psi^{-1}\right] \quad \text{(A5)}$$

with the additional condition $\lim_{\xi\to\infty}\tilde{b}(\xi) = 0$ replacing the crack closure condition that appears in the second Eq. (A2). As discussed by Rubinstein (1992), this representation stabilizes the singular integral equation. $w(\xi)$ is a function of the type

$$w(\xi) = \sin^2\left[\frac{\pi}{2}\left(1 - \frac{\delta}{\xi}\right)\right]. \quad \text{(A6)}$$

With the change of variables $\xi = 2\delta/(1-t)$, $y = 2\delta/(1-\zeta)$ (A4) is normalized in the interval $[-1, 1]$.

By extracting the dominant term of the singularity of the resulting equation, the nondimensional ratio of the local and far-field stress intensity factors is determined as

$$f(\alpha, \beta) = \frac{K_I}{k_I}\delta^{\lambda - 1/2} = \tilde{b}(-1). \quad \text{(A7)}$$

Crack of Length $2a$ Extending Through the Interface by $\delta(\delta \geq 0)$

The set of coupled singular integral equations is given in (14) with A_i and K_{ij} defined in (A1). The compatibility condition at the interface is given in (15). The normalized nondimensional form of (14) and (15) is attained by means of the transformations

$$t_1 = \frac{\xi - a}{a}; \quad \zeta_1 = \frac{y-a}{a}; \quad \phi_1 = -\frac{\sigma^{(1)}(1+\kappa_1)}{2\mu_1};$$

$$t_2 = -\frac{\xi + b}{b}; \quad \zeta_2 = -\frac{y+b}{b}; \quad \phi_2 = -\frac{\sigma^{(2)}(1+\kappa_2)}{2\mu_2};$$

that lead to the following representation of the dislocation densities:

$$b^{(1)}(t_1) = \tilde{b}^{(1)}(t_1)(1-t_1)^{-1/2}(1+t_1)^{\mu};$$
$$b^{(2)}(t_2) = \tilde{b}^{(2)}(t_2)(1-t_2)^{-1/2}(1+t_2)^{\mu} \quad \text{(A8)}$$

where

$$c = b/a.$$

The nondimensional stress intensity factor at the crack tip closer to the interface is then given by

$$g^*(\alpha, \beta) = \frac{K_I}{\sigma^{(1)}\sqrt{\pi l}} = -\frac{1}{2^{\mu}\phi_1}\sqrt{\frac{2c}{1+c}}\frac{1+\alpha}{1-\alpha}\tilde{b}^{(2)}(1). \quad \text{(A9)}$$

Semi-infinite Crack Whose Tip is at Distance δ Beyond the Interface

The equations for this case are similar to the first two Eqs. (14) with the upper limit $2a$ replaced with ∞, and Eq. (15). The third Eq. (14) is replaced by the following condition that stabilizes the integral equations and insures uniqueness of the solution:

$$\lim_{\xi\to\infty}\tilde{b}^{(1)}(\xi) = 0.$$

The dislocation density functions have the form

$$b^{(1)}(\xi) = \frac{k_I}{\sqrt{2\pi}}\frac{1}{(\xi+\delta)^{\lambda-\mu}\xi^{\mu}}\left[\frac{\kappa_1+1}{2\mu_1}\tilde{b}^{(1)}(\xi) + w_1(\xi)\psi^{-1}\right]$$

$$b^{(2)}(\xi) = \frac{k_I}{\sqrt{2\pi}}\frac{\kappa_2+1}{2\mu_2}\frac{\tilde{b}^{(2)}(\xi)}{(-\xi)^{\mu}(\delta+\xi)^{1/2}}\delta^{1/2+\mu-\lambda} \quad \text{(A10)}$$

where $w_1(\xi)$ is a function of the type

$$w_1(\xi) = \sin^2\left[\frac{\pi}{2}\frac{\xi+1}{\xi}\right]. \quad \text{(A11)}$$

The normalized form of the set of equations is attained through the change of variables

$$t_1 = \frac{\xi - \delta}{\xi + \delta}; \quad \zeta_1 = \frac{y-\delta}{y+\delta}; \quad t_2 = \frac{2\xi+\delta}{\delta}; \quad \zeta_2 = \frac{2y+\delta}{\delta}.$$

By extracting the dominant term of the crack-tip singularity, the nondimensional ratio of the local and far-field stress intensity factor is then given by

$$f^*(\alpha, \beta) = \frac{K_I}{k_I}\delta^{\lambda - 1/2} = \tilde{b}^{(2)}(1). \quad \text{(A12)}$$

The crack-opening displacement at the interface is given by

$$\eta = -\int_{-\delta}^{0} B_2(\xi)d\xi = \frac{\delta}{2}\int_{-1}^{1} B_2(t_2)dt_2$$
$$= \frac{1+\kappa_1}{2\mu_1}k_I\delta^{1-\lambda}\tilde{\eta}(\alpha, \beta) \quad \text{(A13)}$$